

Study environmental dependence of galaxy properties

Sergei Dodonov¹, Aleksandra Grokhovskaya¹

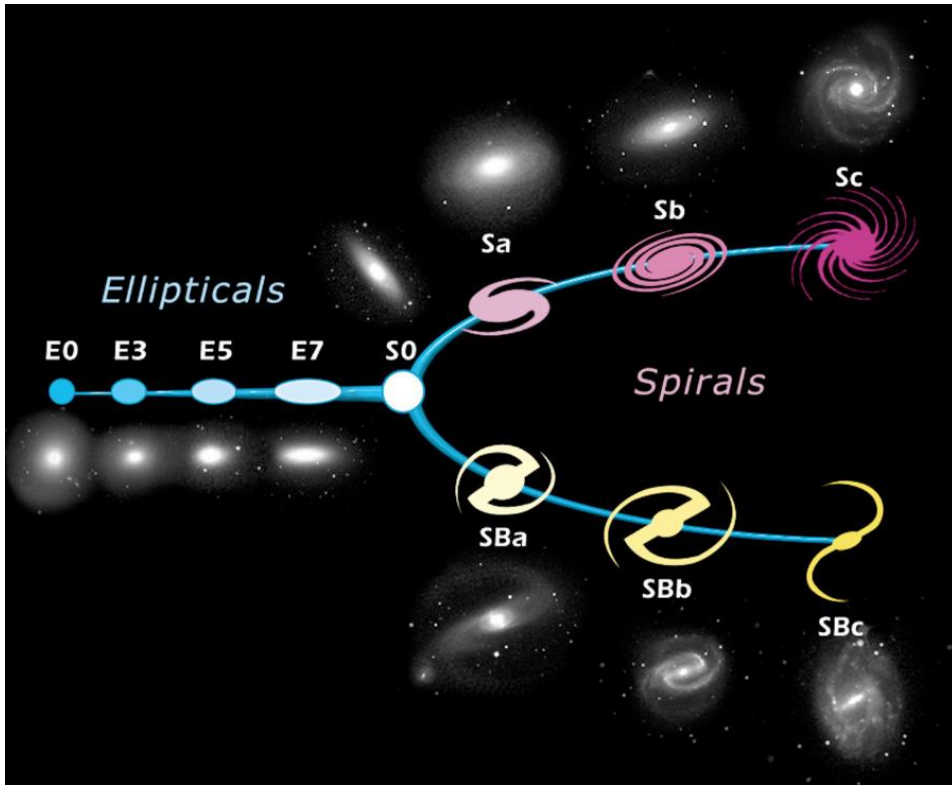
¹ SAO RAS (Special Astrophysical Observatory)





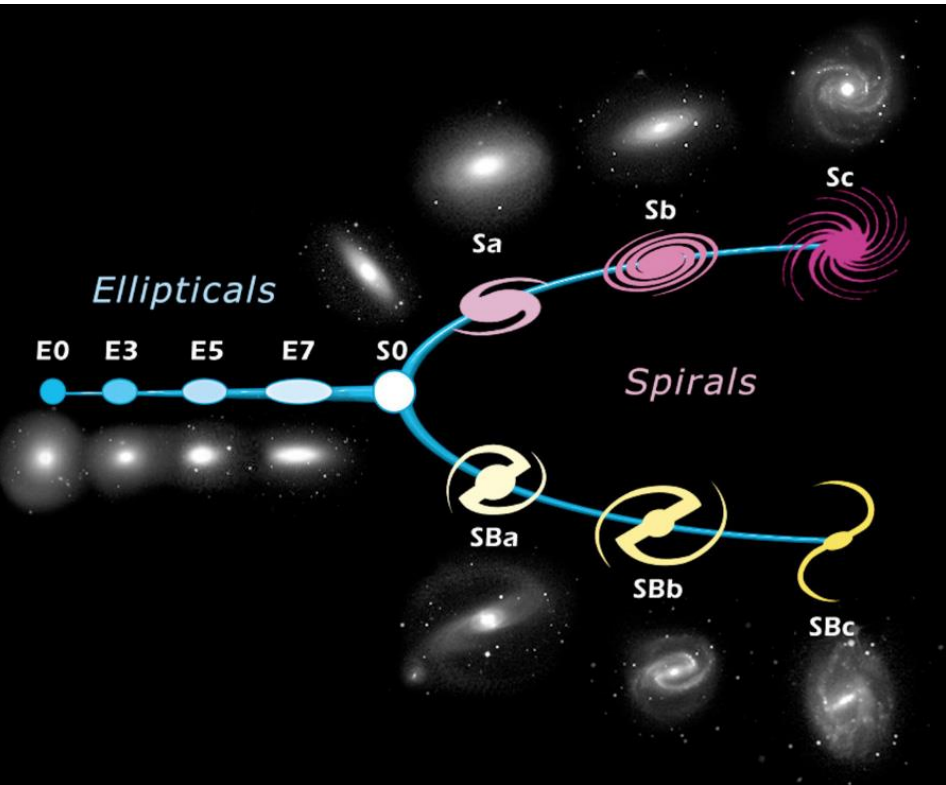
The reasons

Galaxies

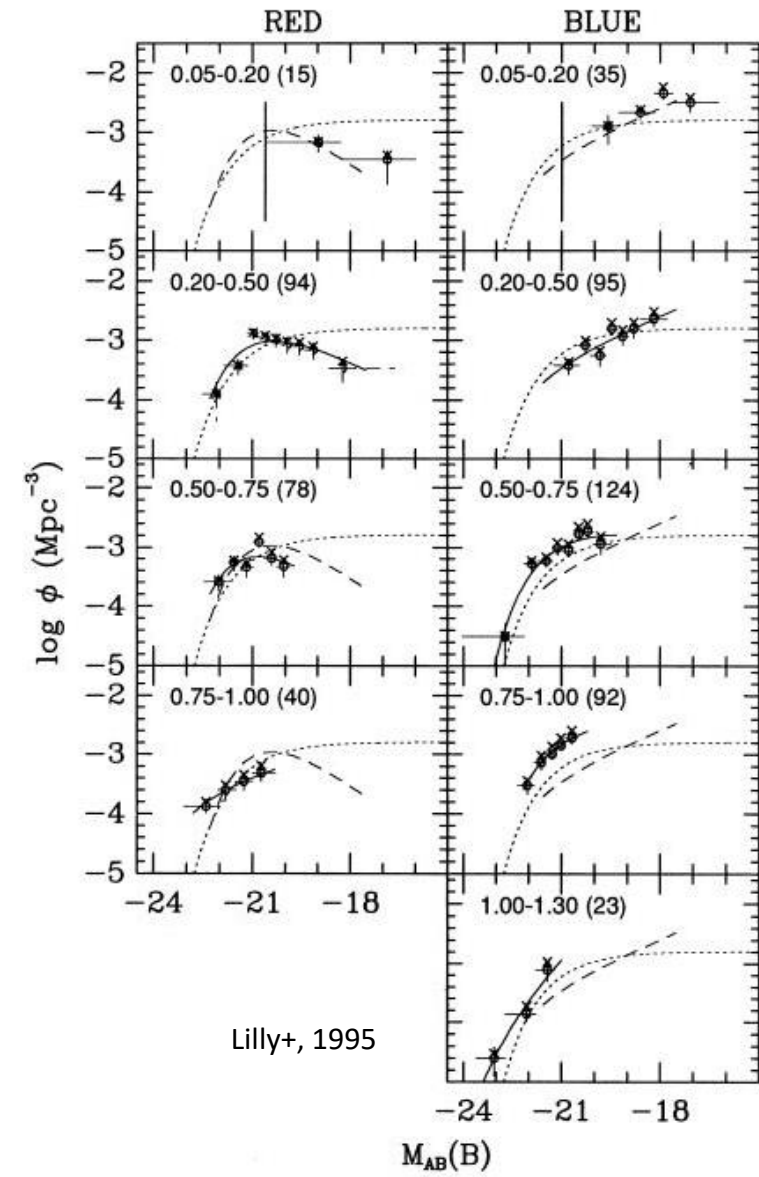


Hubble, 1926



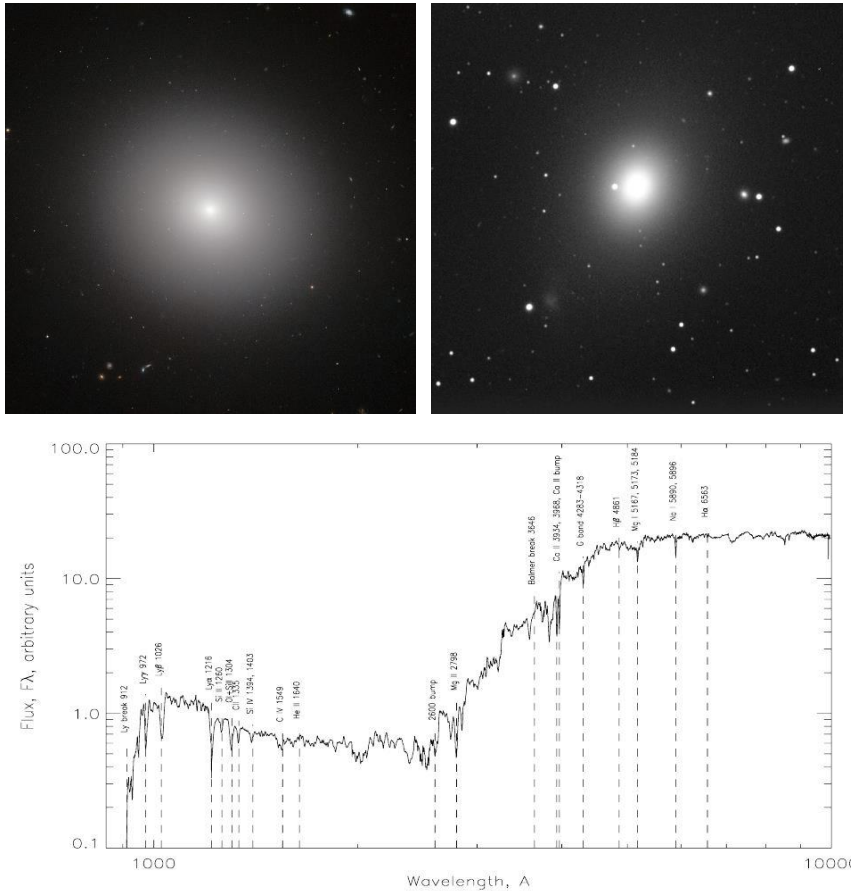


Hubble, 1926



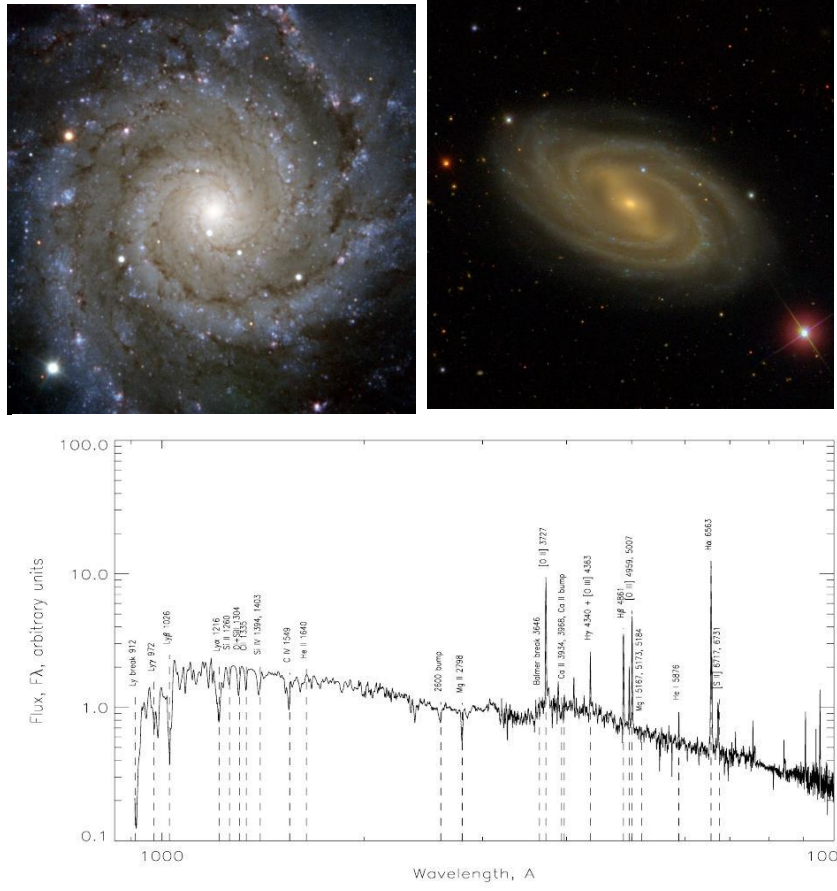


Red galaxies



Composite spectrum of elliptical galaxy

Blue galaxies



Composite spectrum of Sc/SBc/Scd/SBcd galaxy



Morphology - density relation

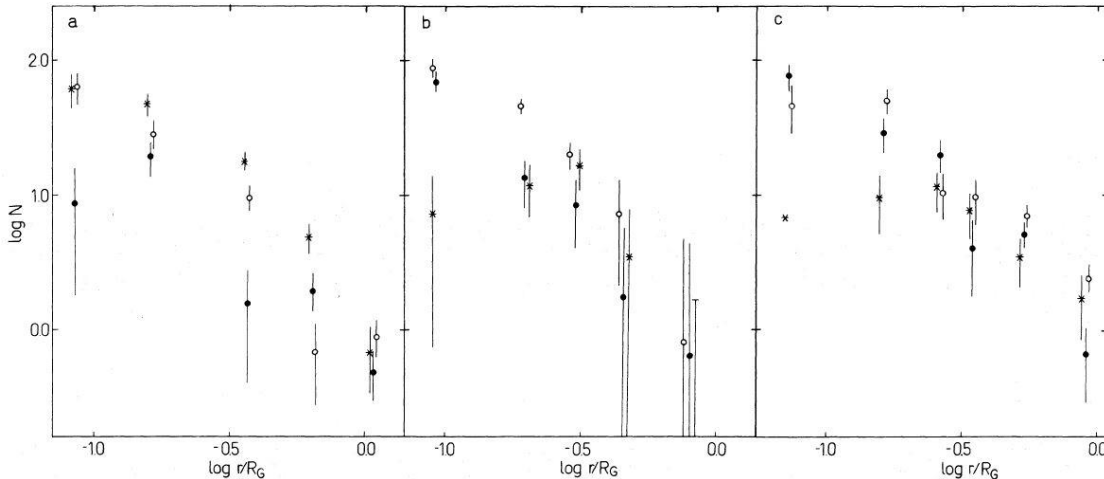


FIG. 9.—Composite projected number density profiles for spiral-rich (a), spiral-poor (b), and cD clusters (c). Spirals are denoted by stars; S0's, by open circles; and ellipticals, by filled circles.

Dresser, 1980

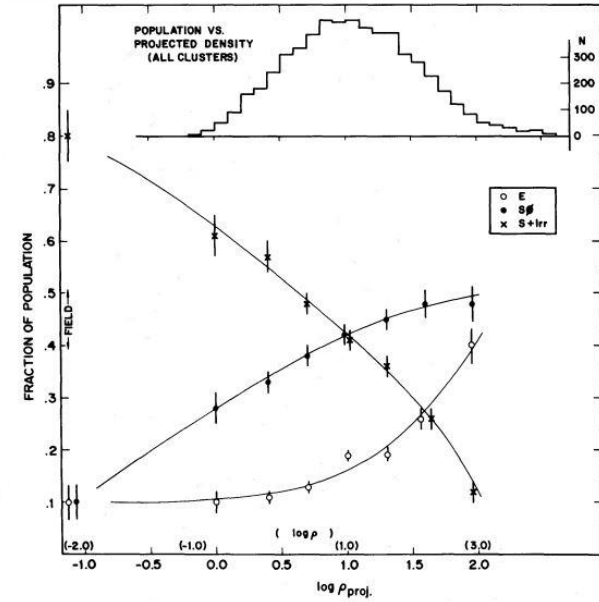


FIG. 4.—The fraction of E, S0, and S+I galaxies as a function of the log of the projected density, in galaxies Mpc^{-2} . The data shown are for all cluster galaxies in the sample and for the field. Also shown is an estimated scale of true space density in galaxies Mpc^{-3} . The upper histogram shows the number distribution of the galaxies over the bins of projected density.

Oemler, 1974



Morphology - density relation

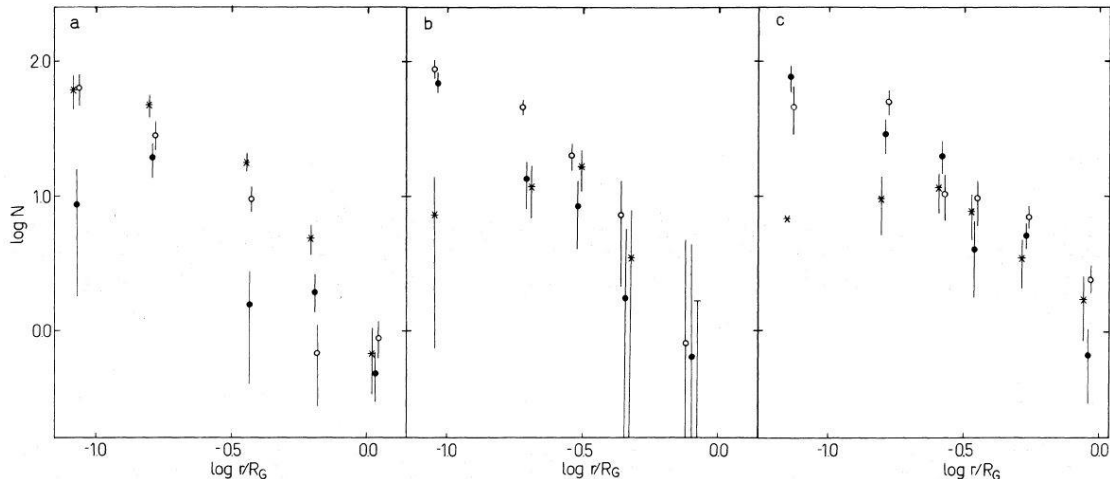
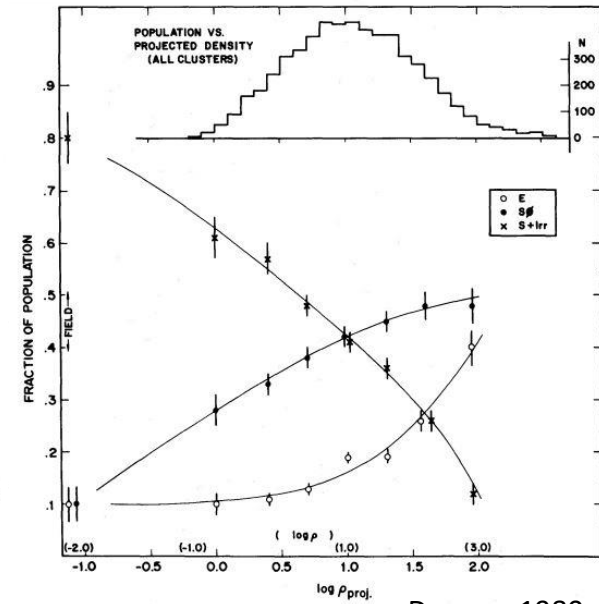
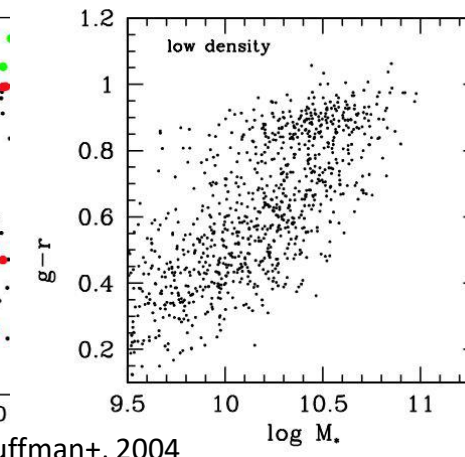
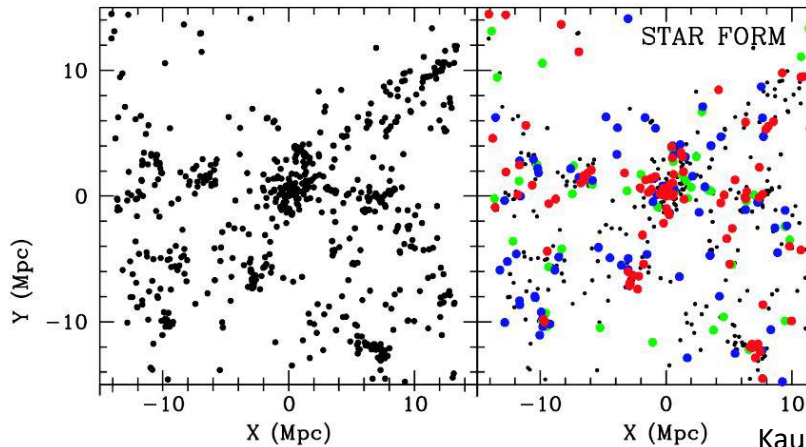


FIG. 9.—Composite projected number density profiles for spiral-rich (a), spiral-poor (b), and cD clusters (c). Spirals are denoted by stars; S0's, by open circles; and ellipticals, by filled circles.

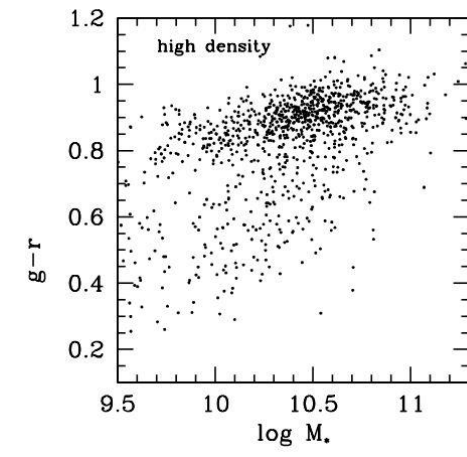
Oemler, 1974



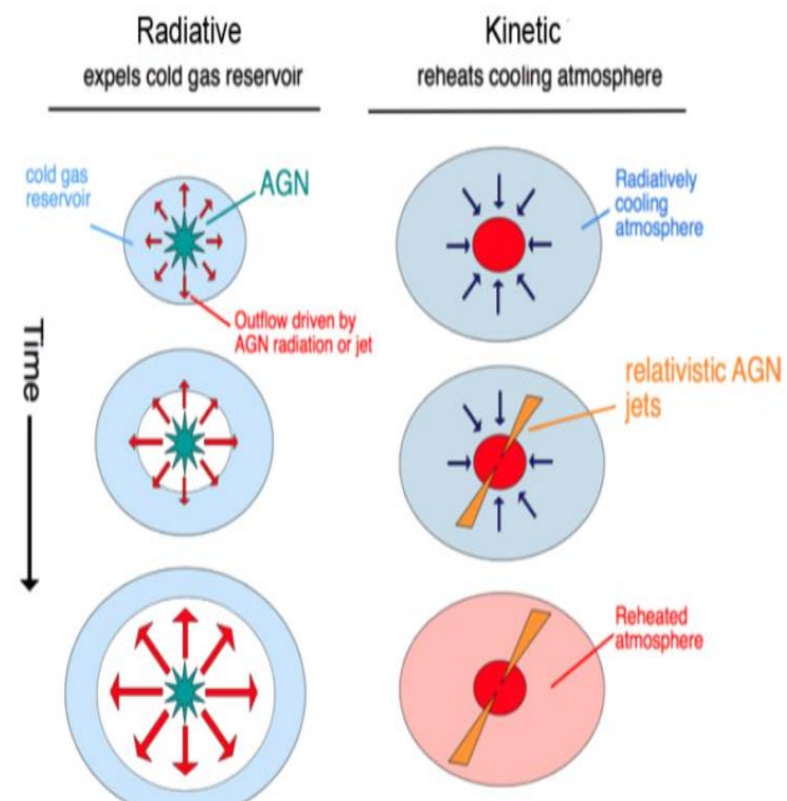
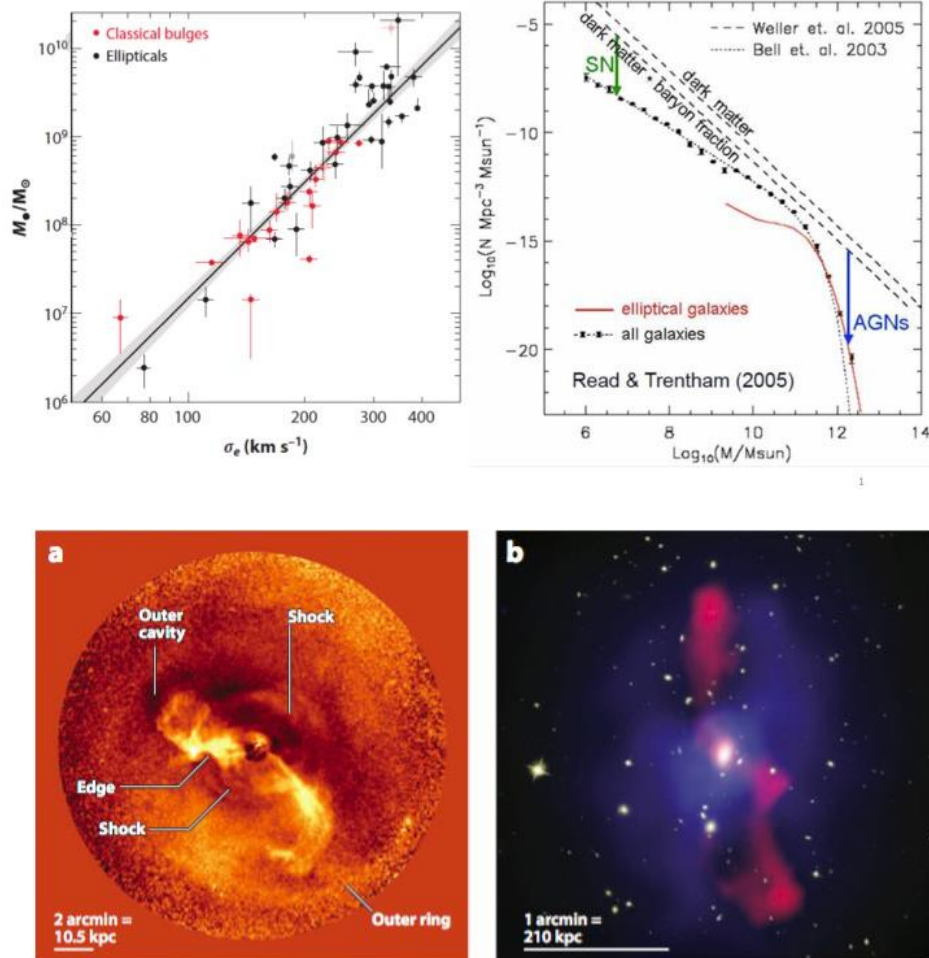
Dresser, 1980



Kauffmann+, 2004



Feedback





How AGNs can acts on physical parameters in galaxy clusters?



The observations

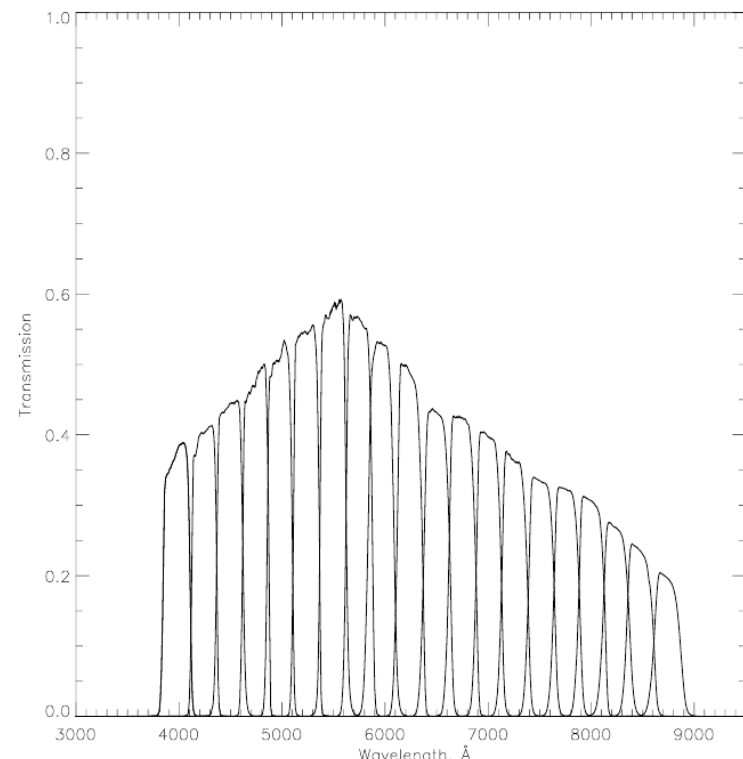


Observations on 1-m Schmidt Telescope



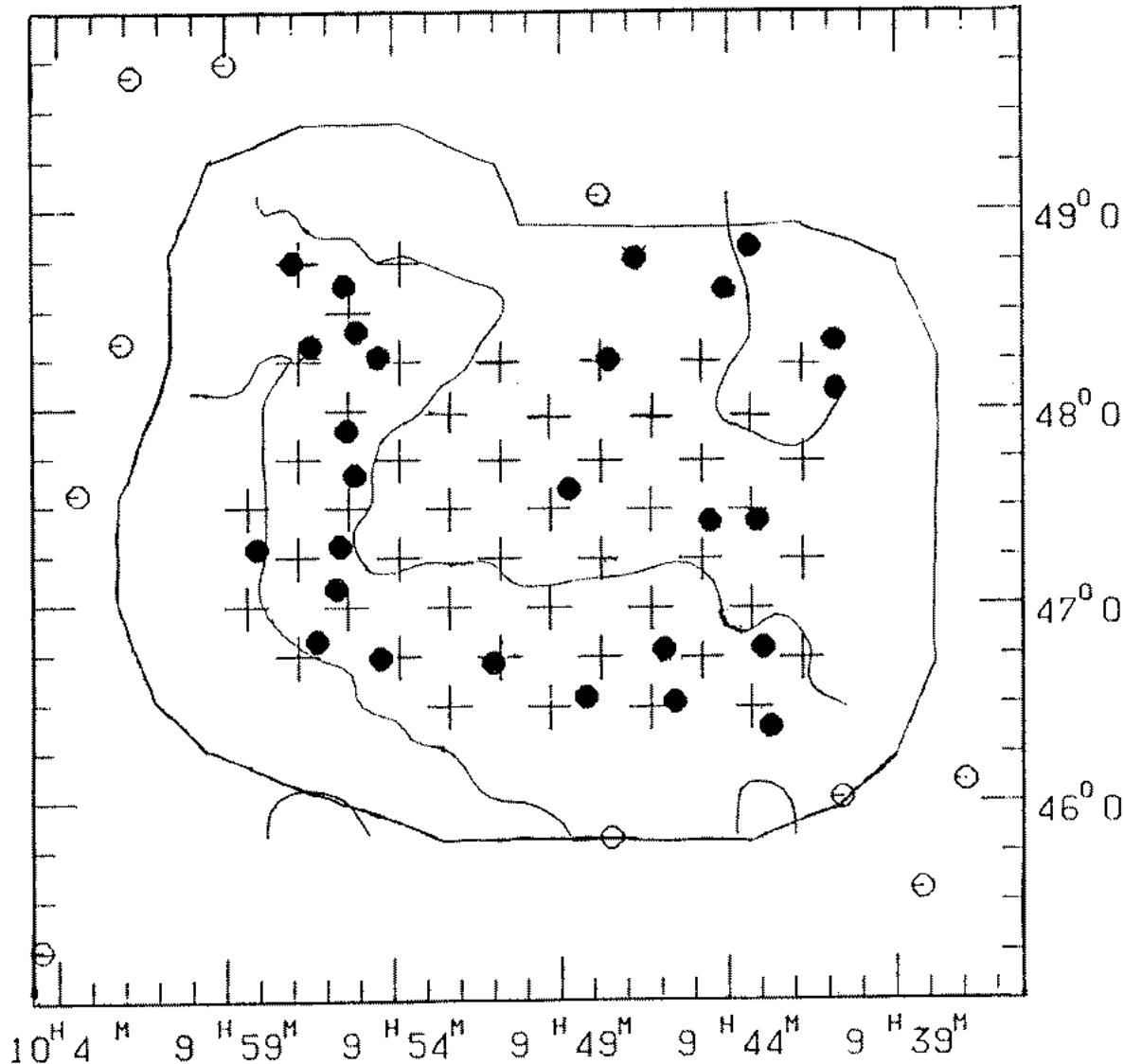
Telescope field of view with 4k x 4k CCD 58 x 58 arcmin, scale 0.868 arcsec/pixel.
 Observations were in four broad band filters (u, g, r and i SDSS) and in 15 medium band (FWHM=250 Å) filters. Total exposure time in filters were varied from 60 min to 120 min depending from the spectral sensitivity of the CCD.

Filter	λ_{cen} , Å	FWHM (Å)	$m_{lim,5\sigma}$
u_SDSS	3578	338	24.23
g_SDSS	4797	860	25.22
r_SDSS	6227	770	24.97
i_SDSS	7624	857	24.15
MB_400	3978	250	24.37
MB_425	4246	250	24.31
MB_450	4492	250	24.20
MB_475	4745	250	24.31
MB_500	4978	250	24.30
MB_525	5234	250	24.37
MB_550	5496	250	23.86
MB_575	5746	250	24.29
MB_600	5959	250	23.89
MB_625	6234	250	23.51
MB_650	6499	250	23.41
MB_675	6745	250	23.78
MB_700	7002	250	23.47
MB_725	7253	250	23.20
MB_750	7519	250	23.07
MB_775	7758	250	22.97



Medium band filters set used in observations.
 CCD spectral response included.

ROSAT survey in the HQS field HS47.5-22



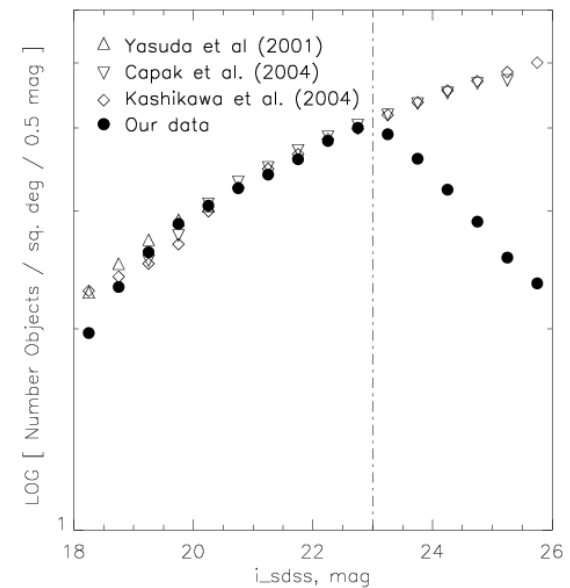
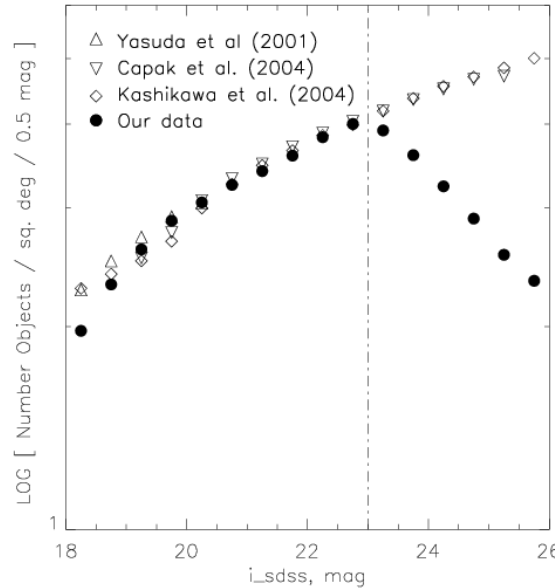
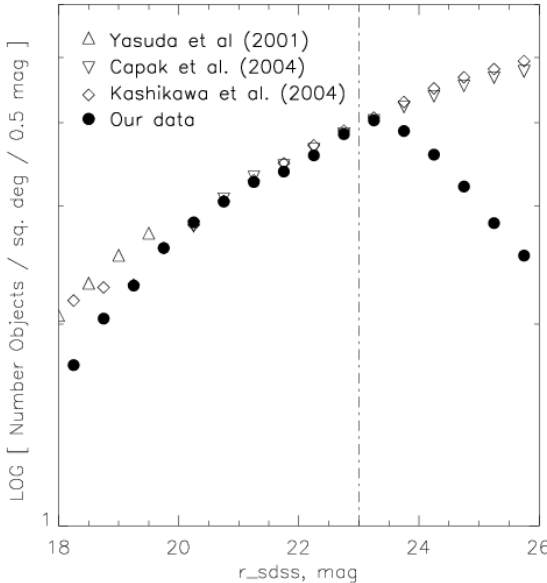
48 overlapping
PSPC pointings

574 X-ray sources

K. Molthagen+, 1997



Galaxies sample definition



Galaxies sample is extracted from the full catalog of objects (near 100000 objects) using following criteria :

- Objects brighter then $\text{RAB}=23\text{m}$;
- Extended index < 0.8 ;
- Index of contamination ≤ 2 .

Into the final sample follow first two criteria we include 39669 objects and after applying third one - we have 36447 objects with clean photometry. Due to the contamination we lose 8.12 % of the objects.

We check sample completeness using comparison of galaxies number-counts in g, r and i SDSS filters from our sample with already published data.



HS47.5-22

RA = $09^{\text{h}}50^{\text{m}}00^{\text{s}}$
DEC = $+47^{\circ}35^{\text{m}}00^{\text{s}}$

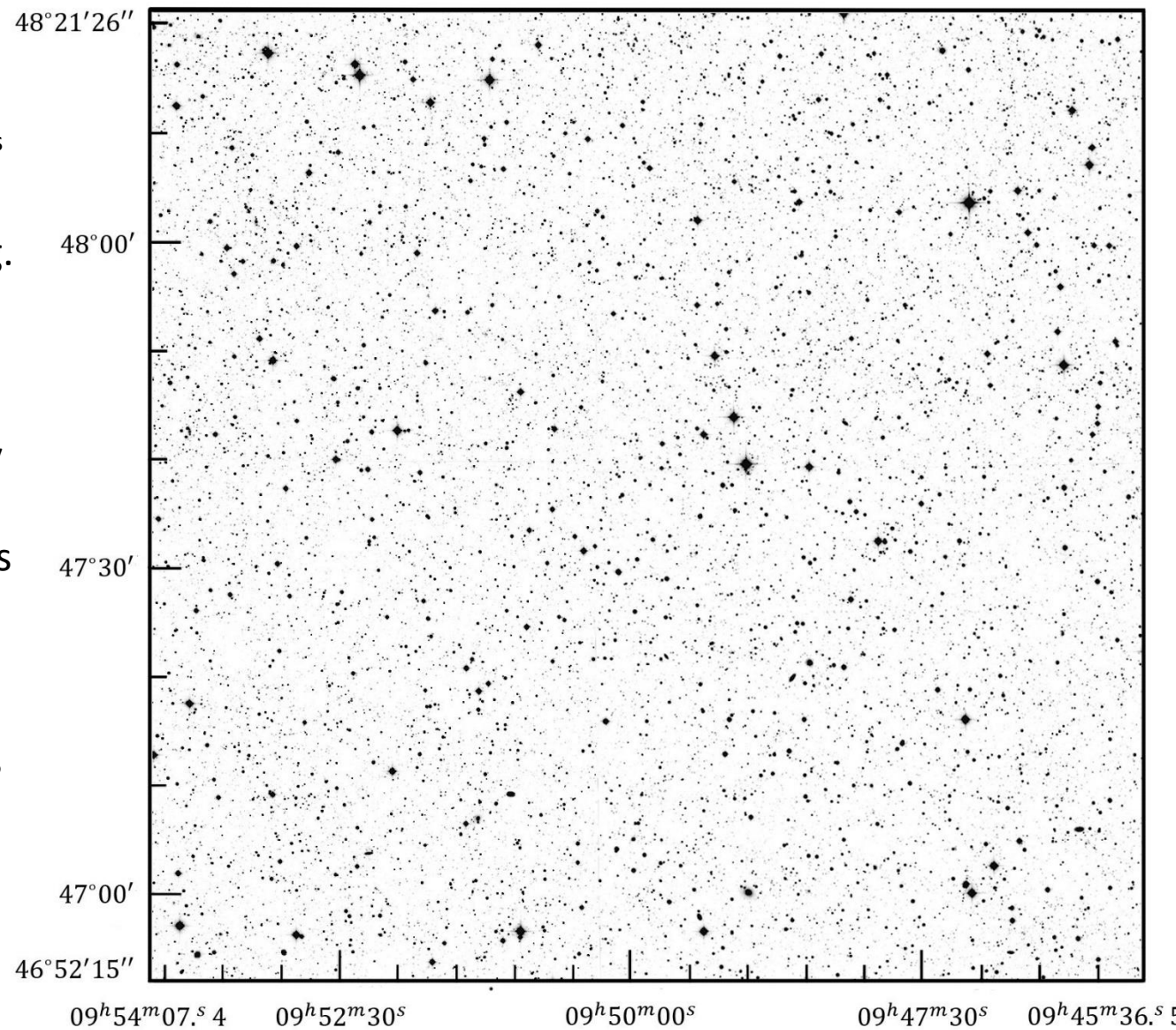
Field 2.39 sq. deg.

36447 Galaxies
to $R_{\text{AB}}=23^{\text{m}}$ with
clean photometry

574 ROSAT Objects
to 3.5×10^{-14} ergs
 $\text{cm}^{-2}\text{s}^{-1}$

362 FIRST Objects

293 SDSS QSO



SEDs Analysis

The photometric measurements from filters set provide low resolution spectra for each object which are analyzed by a statistical technique for classification and redshift estimation based on spectral template matching.

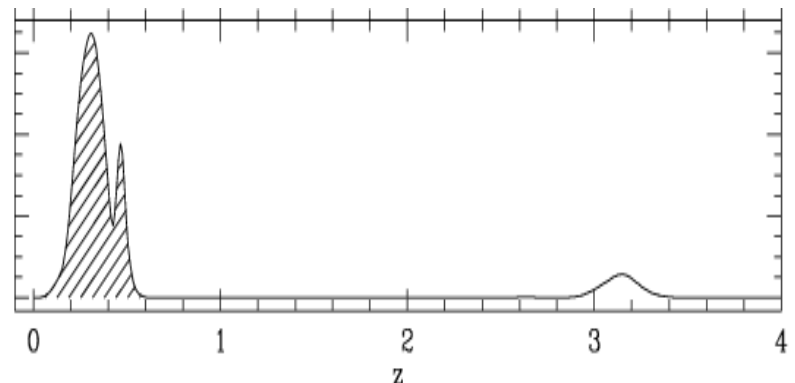
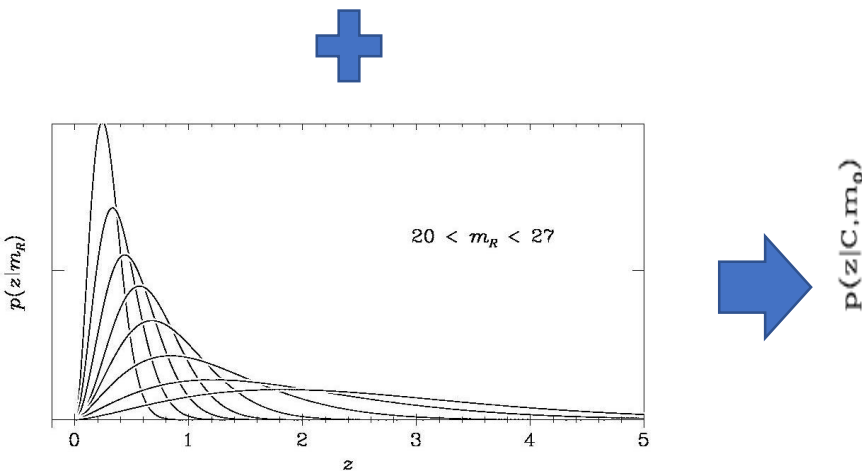
For SEDs analysis should be used :

- Stellar spectra library;
 - Galaxies spectra library;
 - QSO's spectra library.

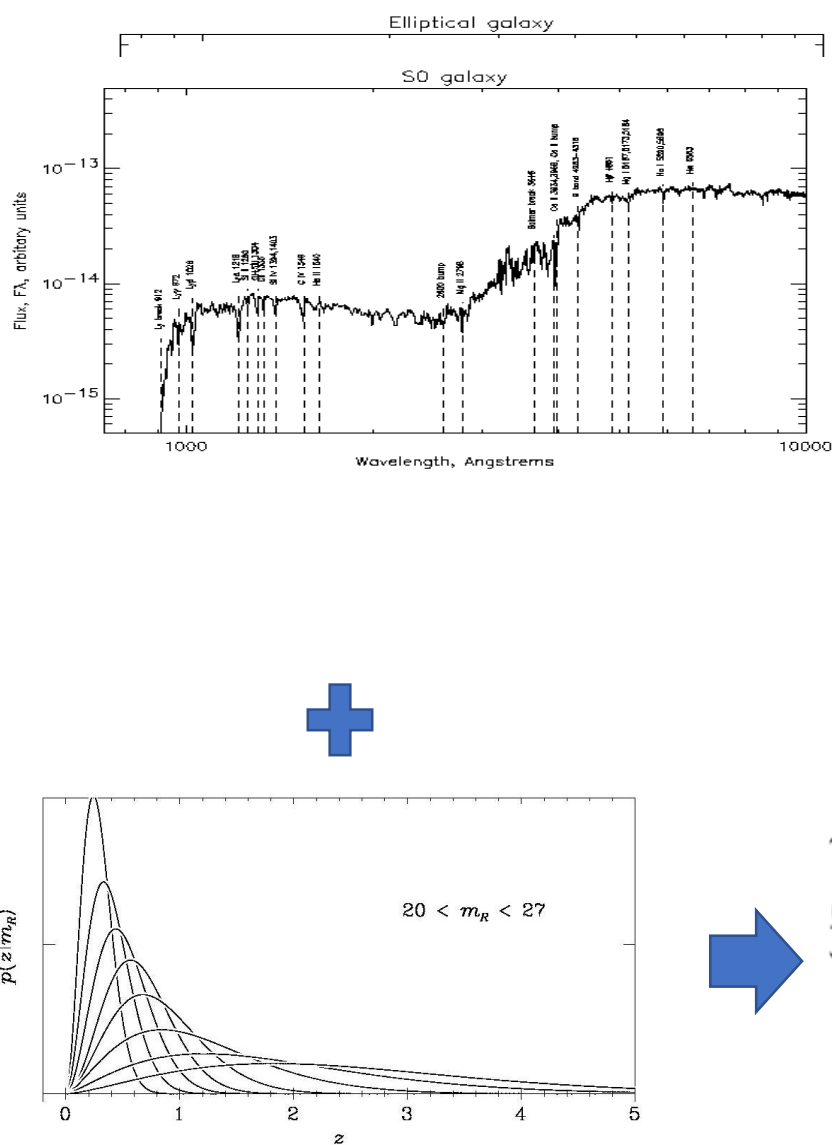
Priors for a galaxy with given magnitude having redshift Z.

Star – Galaxy morphology classification index.

As a result we get a probability that object with given SED classified as galaxy or QSO, or Star with known spectral type and redshift.



SEDs Analysis



The photometric measurements from filters set provide low resolution spectra for each object which are analyzed by a statistical technique for classification and redshift estimation based on spectral template matching.

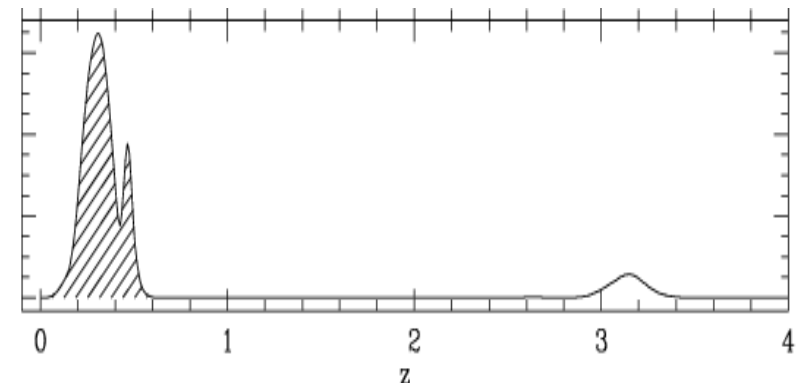
For SEDs analysis should be used :

- Stellar spectra library;
 - Galaxies spectra library;
 - QSO's spectra library.

Priors for a galaxy with given magnitude having redshift Z.

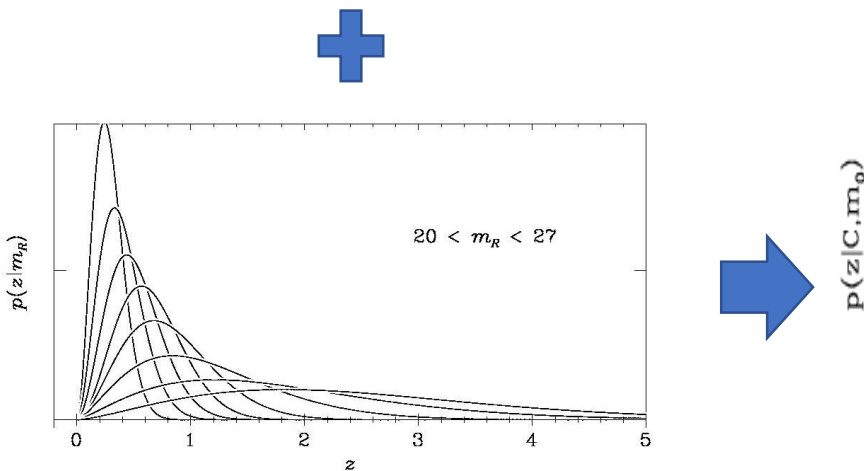
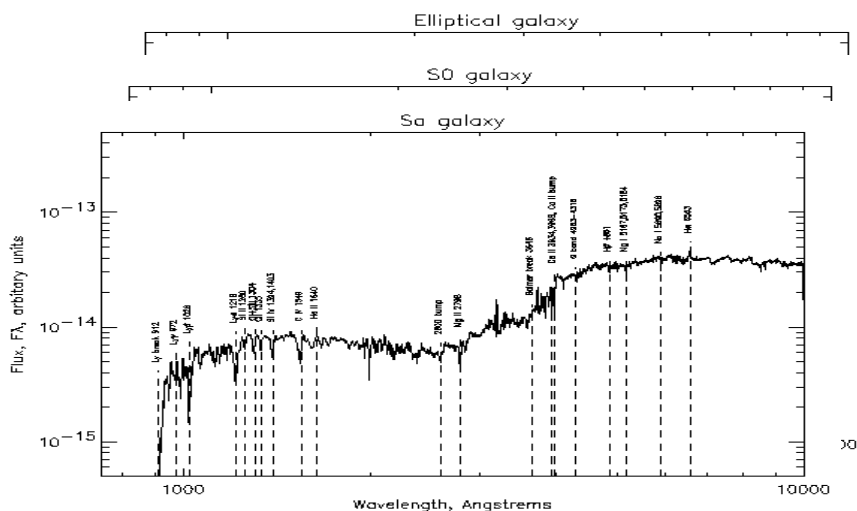
Star – Galaxy morphology classification index.

As a result we get a probability that object with given SED classified as galaxy or QSO, or Star with known spectral type and redshift.





SEDs Analysis



The photometric measurements from filters set provide low resolution spectra for each object which are analyzed by a statistical technique for classification and redshift estimation based on spectral template matching.

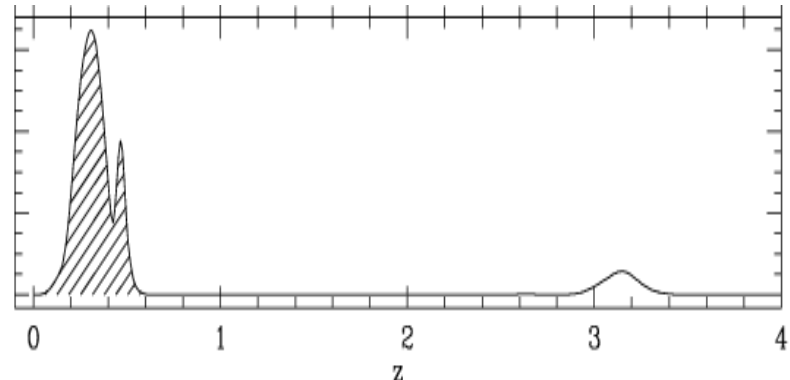
For SEDs analysis should be used :

- Stellar spectra library;
- Galaxies spectra library;
- QSO's spectra library.

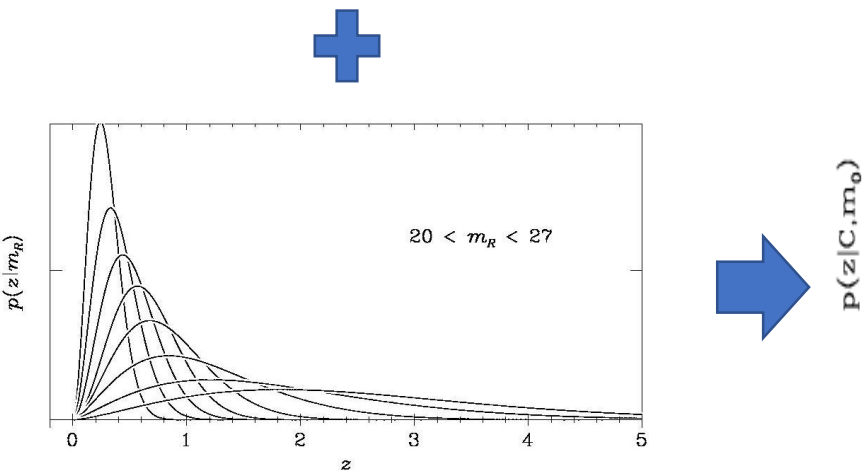
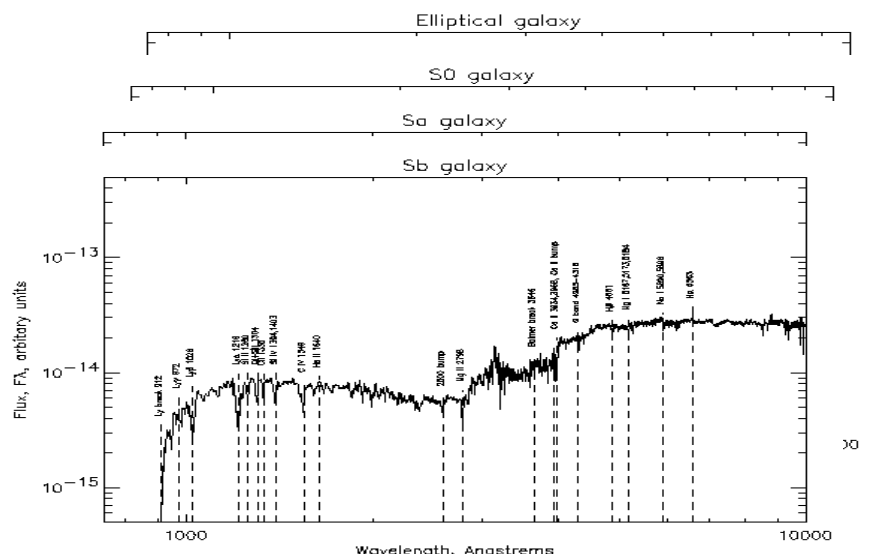
Priors for a galaxy with given magnitude having redshift Z.

Star – Galaxy morphology classification index.

As a result we get a probability that object with given SED classified as galaxy or QSO, or Star with known spectral type and redshift.



SEDs Analysis



The photometric measurements from filters set provide low resolution spectra for each object which are analyzed by a statistical technique for classification and redshift estimation based on spectral template matching.

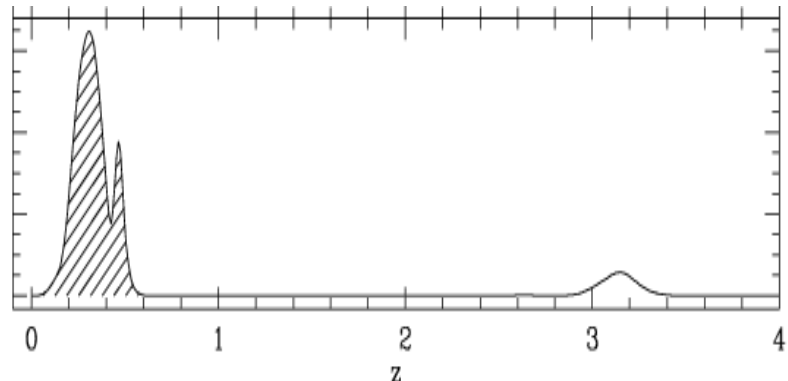
For SEDs analysis should be used :

- Stellar spectra library;
 - Galaxies spectra library;
 - QSO's spectra library.

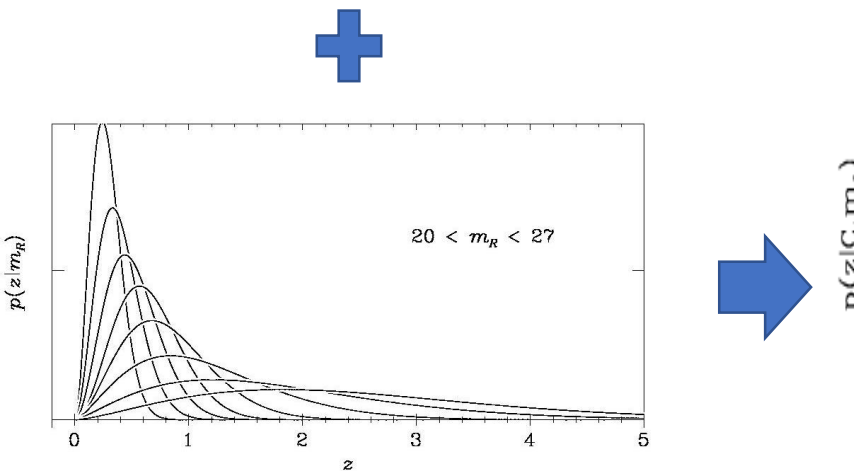
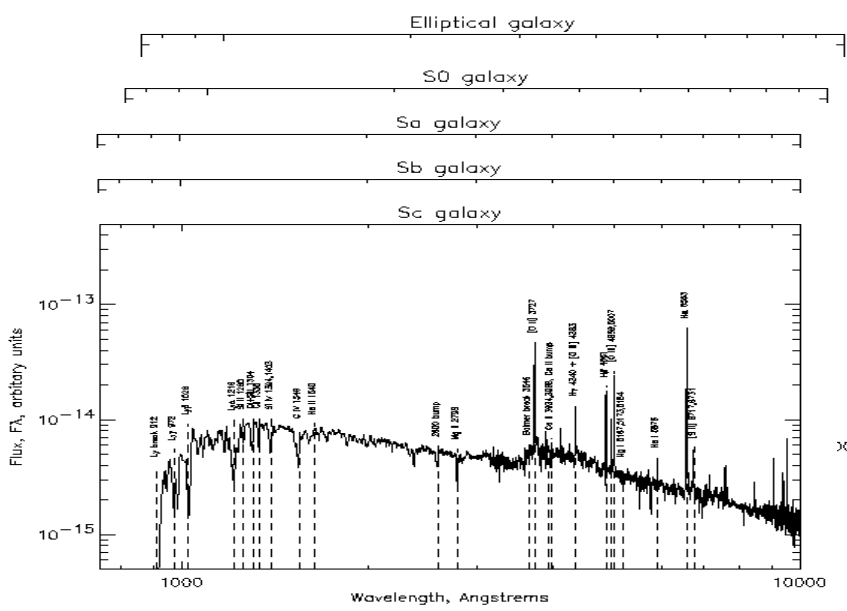
Priors for a galaxy with given magnitude having redshift Z.

Star – Galaxy morphology classification index.

As a result we get a probability that object with given SED classified as galaxy or QSO, or Star with known spectral type and redshift.



SEDs Analysis



The photometric measurements from filters set provide low resolution spectra for each object which are analyzed by a statistical technique for classification and redshift estimation based on spectral template matching.

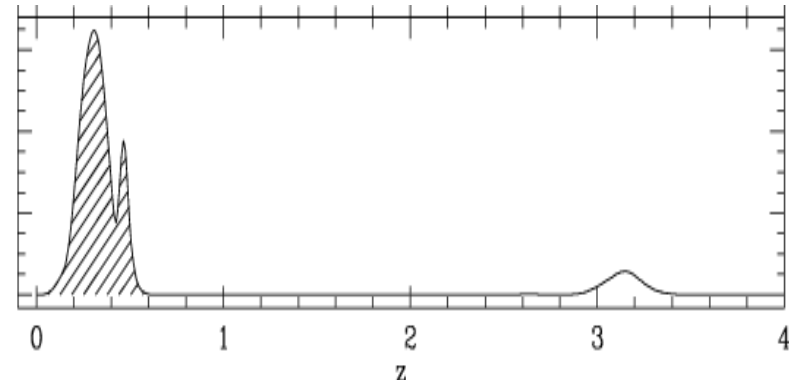
For SEDs analysis should be used :

- Stellar spectra library;
 - Galaxies spectra library;
 - QSO's spectra library.

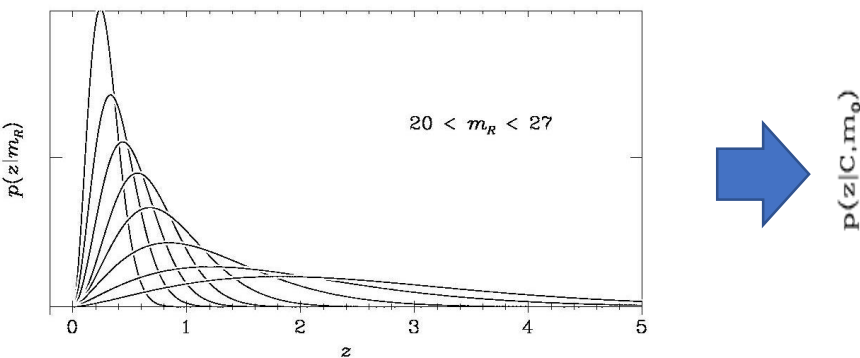
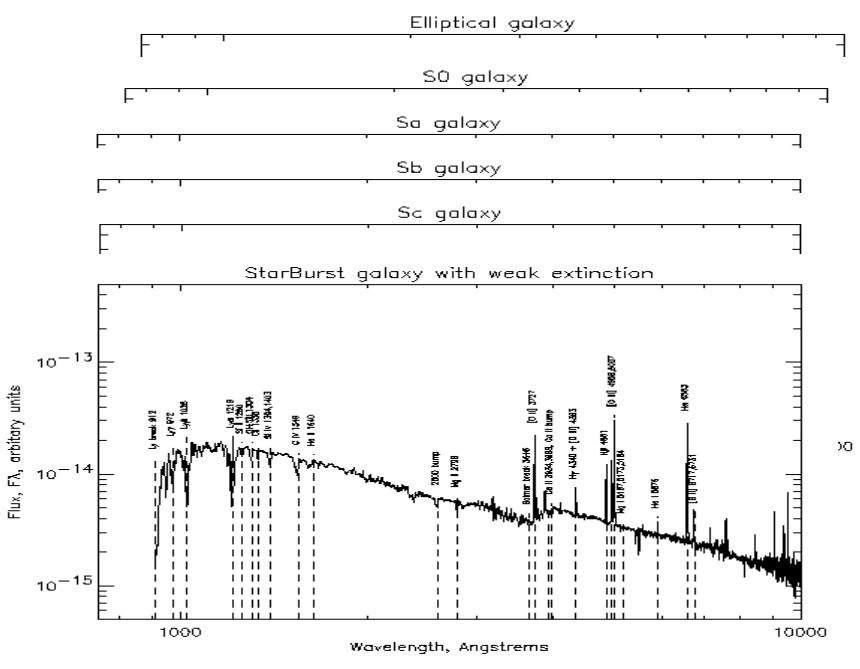
Priors for a galaxy with given magnitude having redshift Z.

Star – Galaxy morphology classification index.

As a result we get a probability that object with given SED classified as galaxy or QSO, or Star with known spectral type and redshift.



SEDs Analysis



The photometric measurements from filters set provide low resolution spectra for each object which are analyzed by a statistical technique for classification and redshift estimation based on spectral template matching.

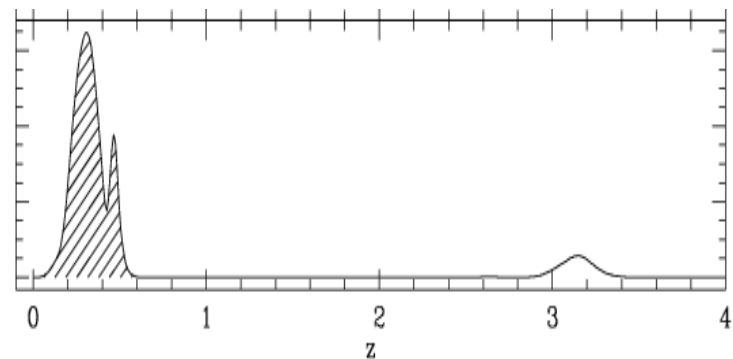
For SEDs analysis should be used :

- Stellar spectra library;
 - Galaxies spectra library;
 - QSO's spectra library.

- Priors for a galaxy with given magnitude having redshift Z.

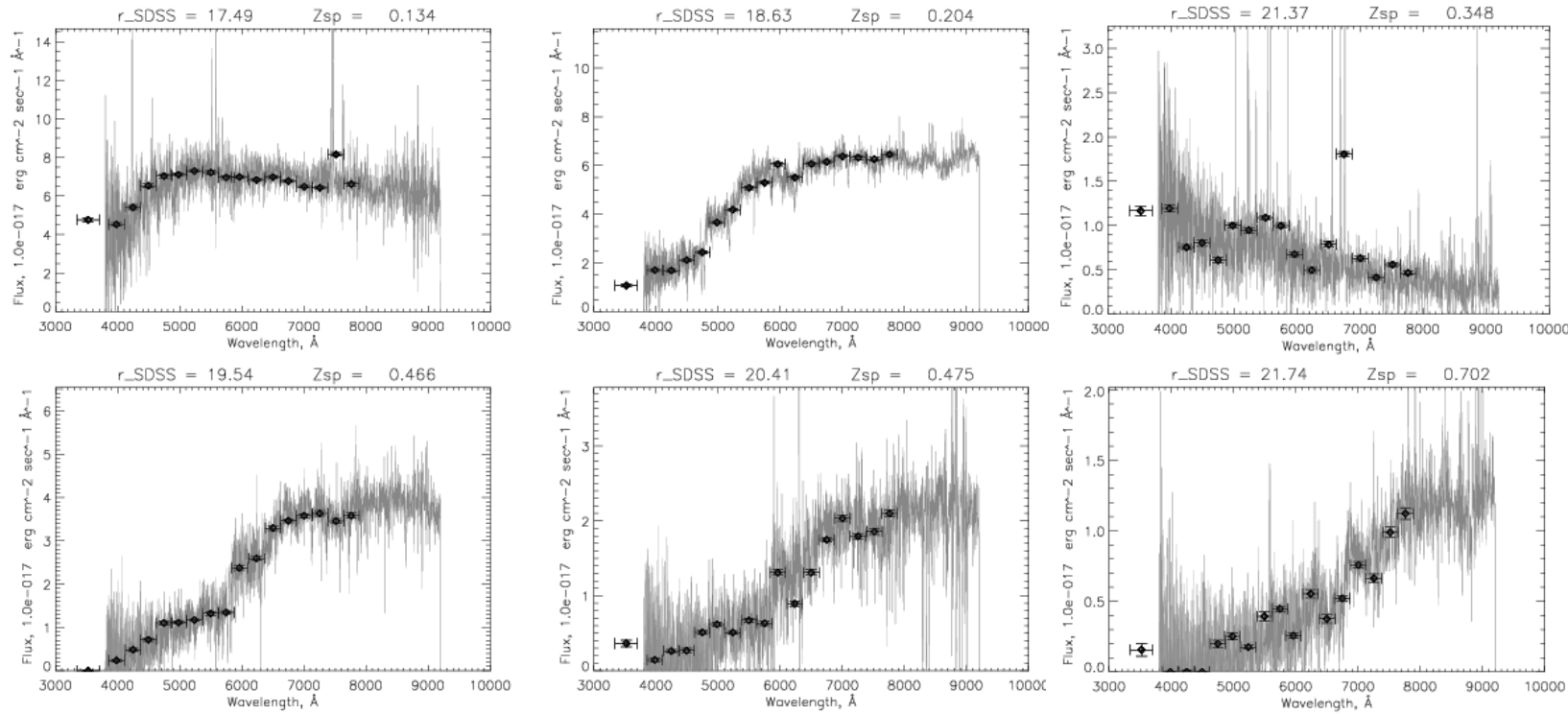
Star – Galaxy morphology classification index.

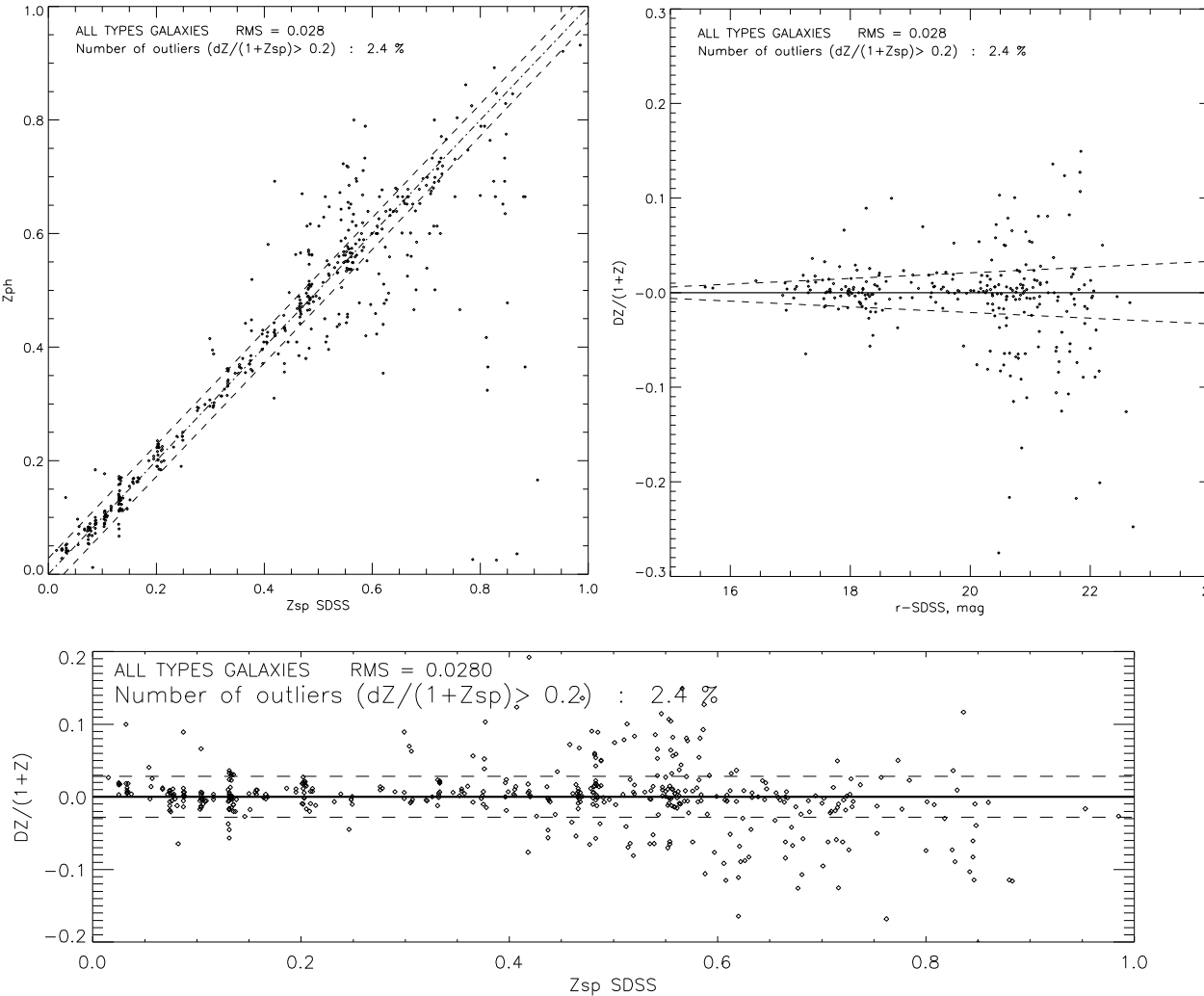
As a result we get a probability that object with given SED classified as galaxy or QSO, or Star with known spectral type and redshift.





Spectral Energy Distribution vs SDSS Spectra





Comparison between photometric redshifts Z_{ph} obtained with ZEBRA in Maximum Likelihood mode with SDSS spectroscopic redshifts Z_{sp} along with error distribution $\Delta Z/(1+Z)$ for all galaxies with known spectroscopic redshifts.

Obtained accuracy $\sigma z < 0.028$ and fraction of catastrophic outliers ($\Delta Z/(1+Z) > 0.2$) $\sim 2.4\%$. Accuracy σz changes from 0.011 in magnitude range $r_{\text{SDSS}} = 16\text{m} - 20\text{m}$ till 0.066 in magnitude range $r_{\text{SDSS}} = 21\text{m} - 23\text{m}$.

HS 47.5 + 22 is deep wide homogeneous field (2.386 sq. deg.)
with determined x-ray and radio sources in the field
There is only one more the same field (COSMOS field)





The data analysis

Group and clusters of galaxies. First catalogs

THE DISTRIBUTION OF RICH CLUSTERS OF GALAXIES*

GORGEOUS ABELL†

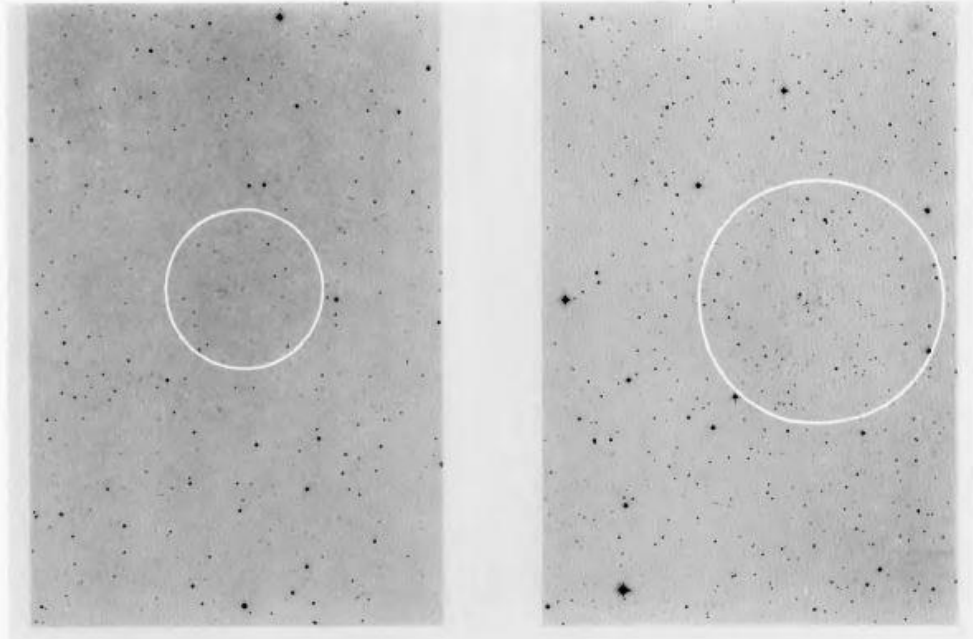
Mount Wilson and Palomar Observatories

Carnegie Institution of Washington, California Institute of Technology

Received September 30, 1957; revised November 13, 1957

ABSTRACT

A catalogue is prepared of 2712 rich clusters of galaxies found on the National Geographic Society-Palomar Observatory Sky Survey. From the catalogue, 1682 clusters are selected which meet specific criteria for inclusion in a homogeneous statistical sample. An investigation of the sample leads to the following conclusions: (1) the distribution function rapidly as n decreases; (2) the data allow no significant variation with distance; (3) galactic obscuration of the origin at high northern galactic latitudes around galactic longitude $l = 0^\circ$; (4) the observed random surface distribution of clusters, both when clusters are considered separately and when their distances are considered. An analysis of the distribution of clusters shows that the distribution of clusters of galaxies is similar to the distribution of second-order clusters, that is, clusters of clusters of galaxies. The comparison between the observed distribution and one of complete randomness shows that the observed distribution is significantly different from the random one.





Group and clusters of galaxies. First catalogs

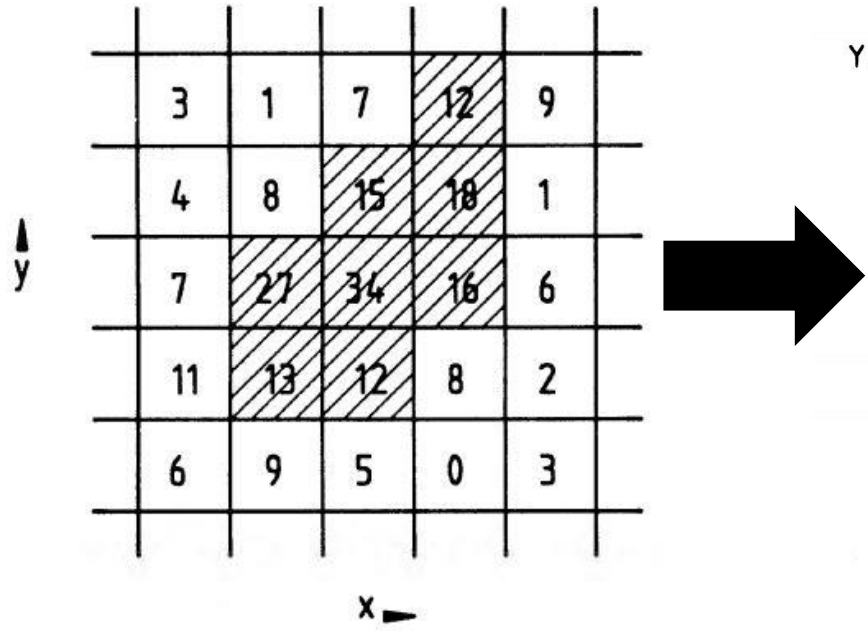


FIG. 1. Subset of galaxy counts from COSMOS scans of a photographic plate with the count resolution being $5' \times 5'$.

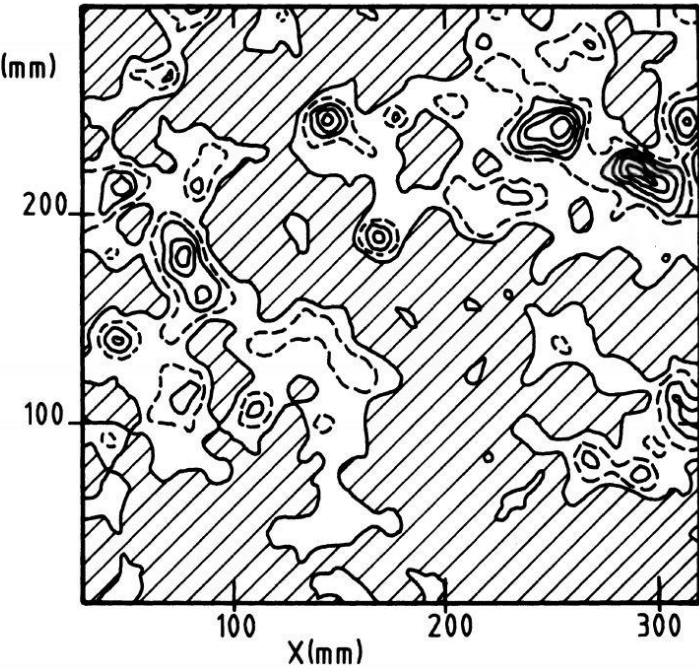
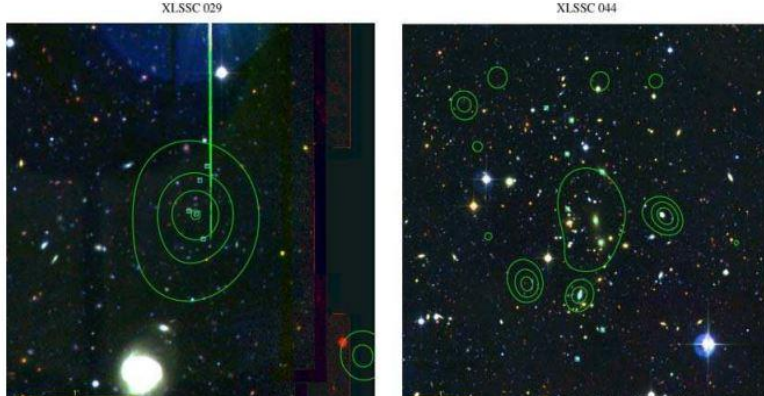


FIG. 2. Distribution of galaxies detected down to $B = 21.5$ in field 411 of the ESO/SERC Southern Sky survey. Hatched areas represent areas of the data in which the galaxy numbers are below the overall mean level of 8 (from counts in $5' \times 5'$). The first isoplethal level is at the mean level, and subsequent isopleths are at intervals of three galaxies per cell thereafter.

Methods

1. X-ray emission from hot gas



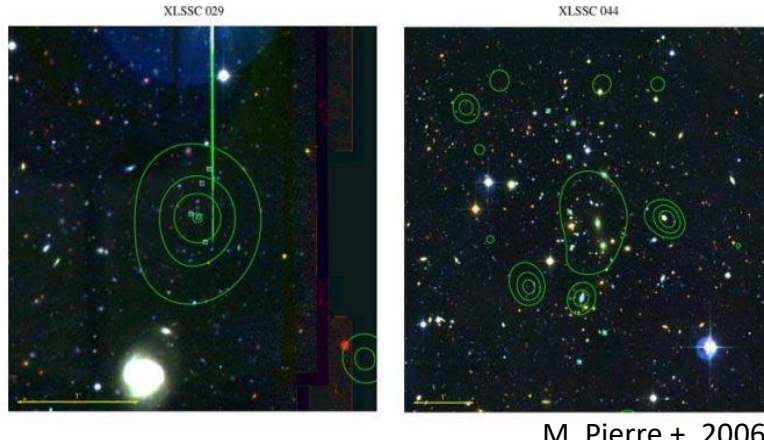
M. Pierre +, 2006





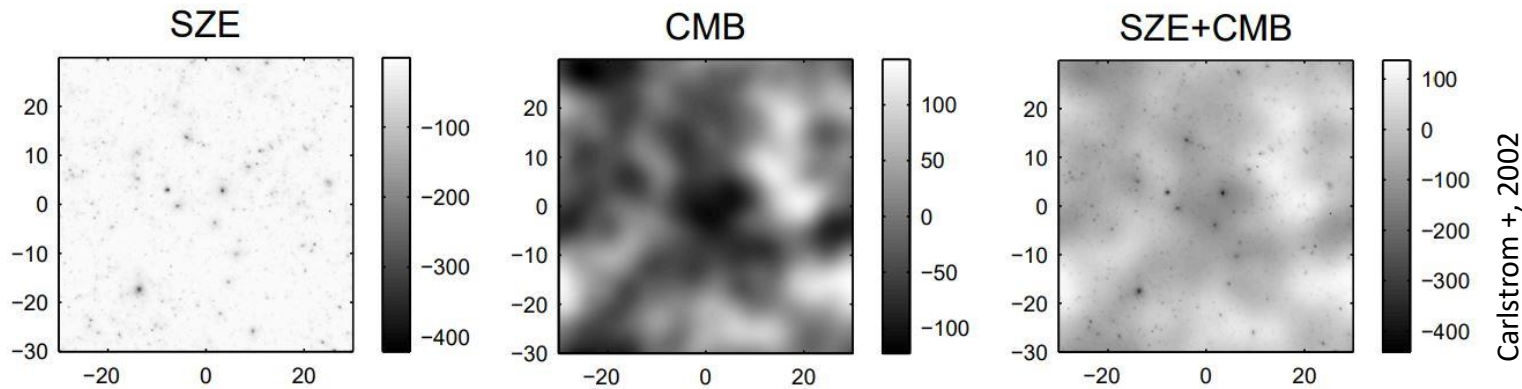
Methods

1. X-ray emission from hot gas



M. Pierre +, 2006

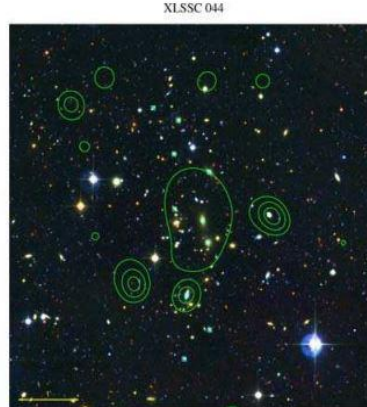
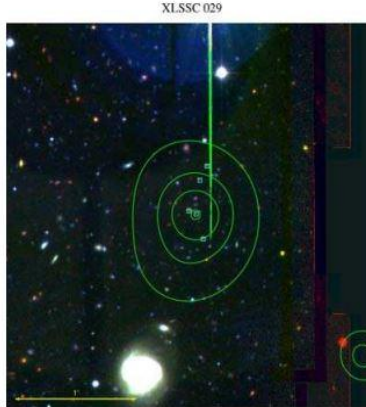
2. Sunyaev–Zel'dovich effect in the CMB





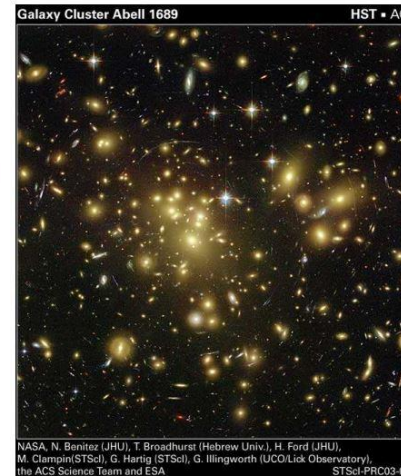
Methods

1. X-ray emission from hot gas

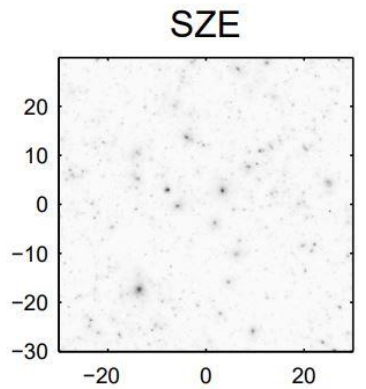


M. Pierre +, 2006

3. Cosmic shear due to weak gravitational lensing



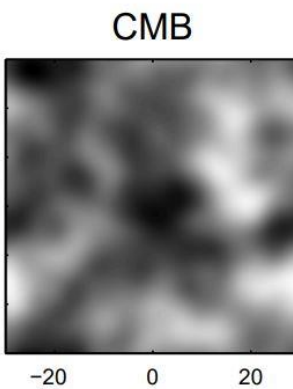
2. Sunyaev–Zel'dovich effect in the CMB



SZE

20
10
0
-10
-20
-30

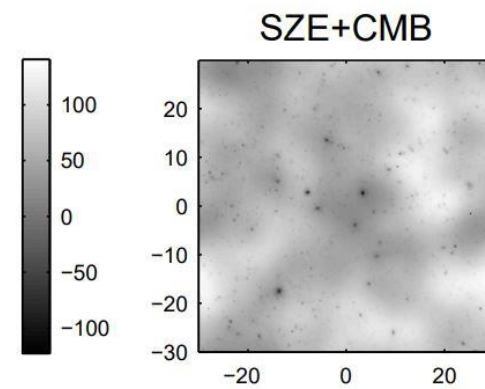
-20 0 20



CMB

20
10
0
-10
-20
-30

-20 0 20



SZE+CMB

100
50
0
-50
-100

-20 0 20

Carlstrom +, 2002

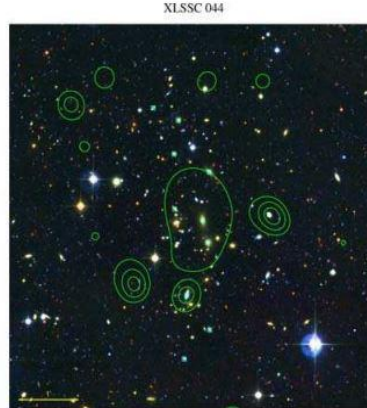
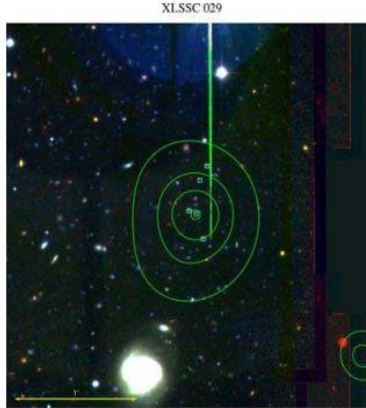
100
50
0
-50
-100

-30



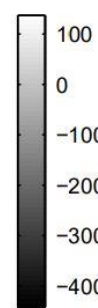
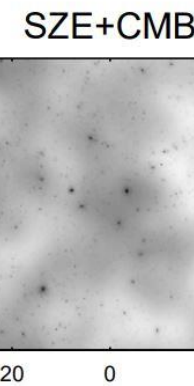
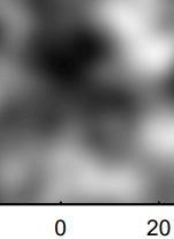
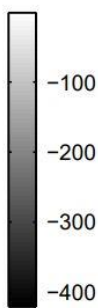
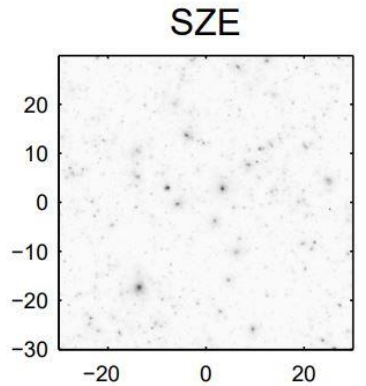
Methods

1. X-ray emission from hot gas

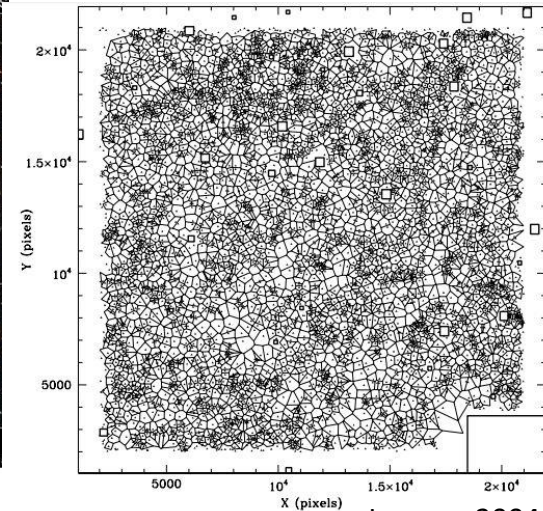
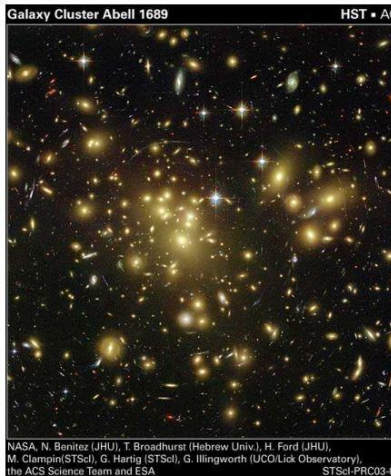


M. Pierre +, 2006

2. Sunyaev–Zel'dovich effect in the CMB



Carlstrom +, 2002



Lopes+, 2004

3. Cosmic shear due to weak gravitational lensing

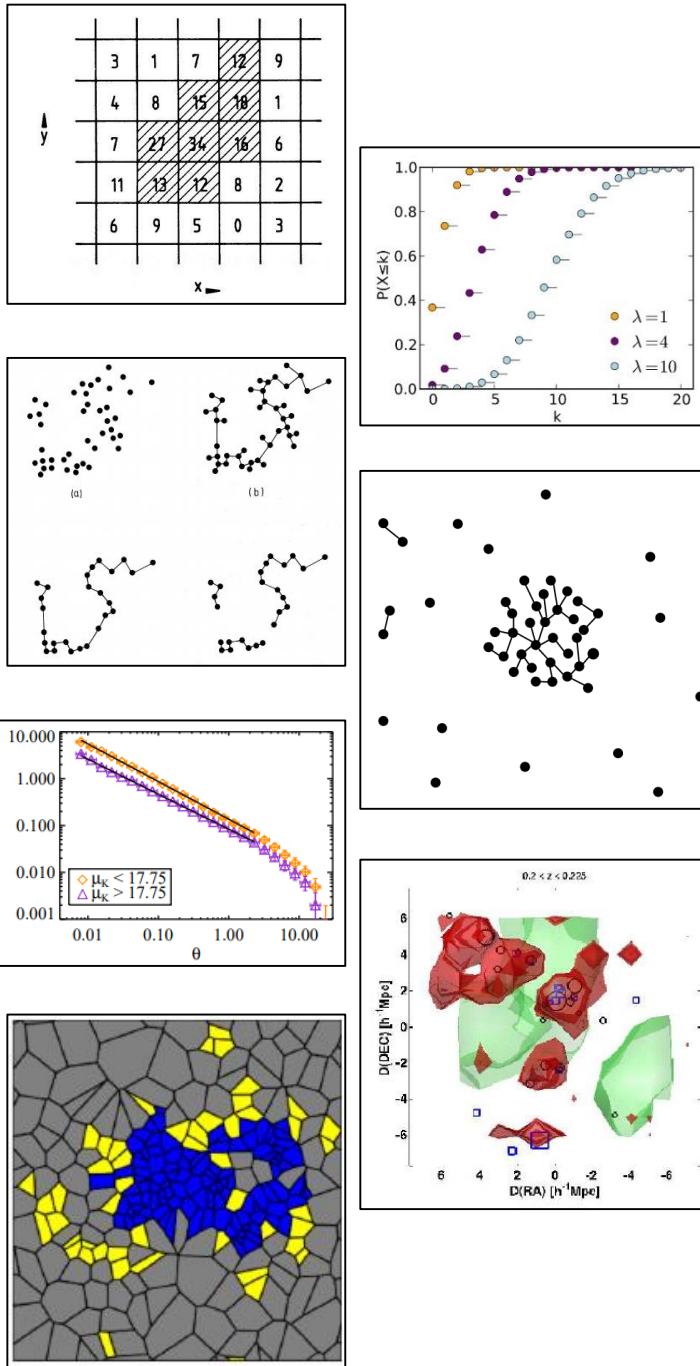
4. Galaxy overdensities in optical, near-infrared or mid-IR images



Algorithms

(short, incomplete, subjective sample)

1. Counting objects projected onto the field
(Shectman +, 1985; Dodd, MacGillivray, 1986)
2. Comparing the distribution functions of objects with Poisson distribution (Limber+, 1953; Neyman & Scott, 1955)
3. Cluster analysis:
 - Minimal spinning tree (Barrow, 1985)
 - Friend-of-friends (More+, 2011)
 - Comparison of correlation functions (Maller+, 2005)
4. Filtering algorithms (Kovac+, 2009)
5. Voronoi diagrams (Ramel+., 2001)





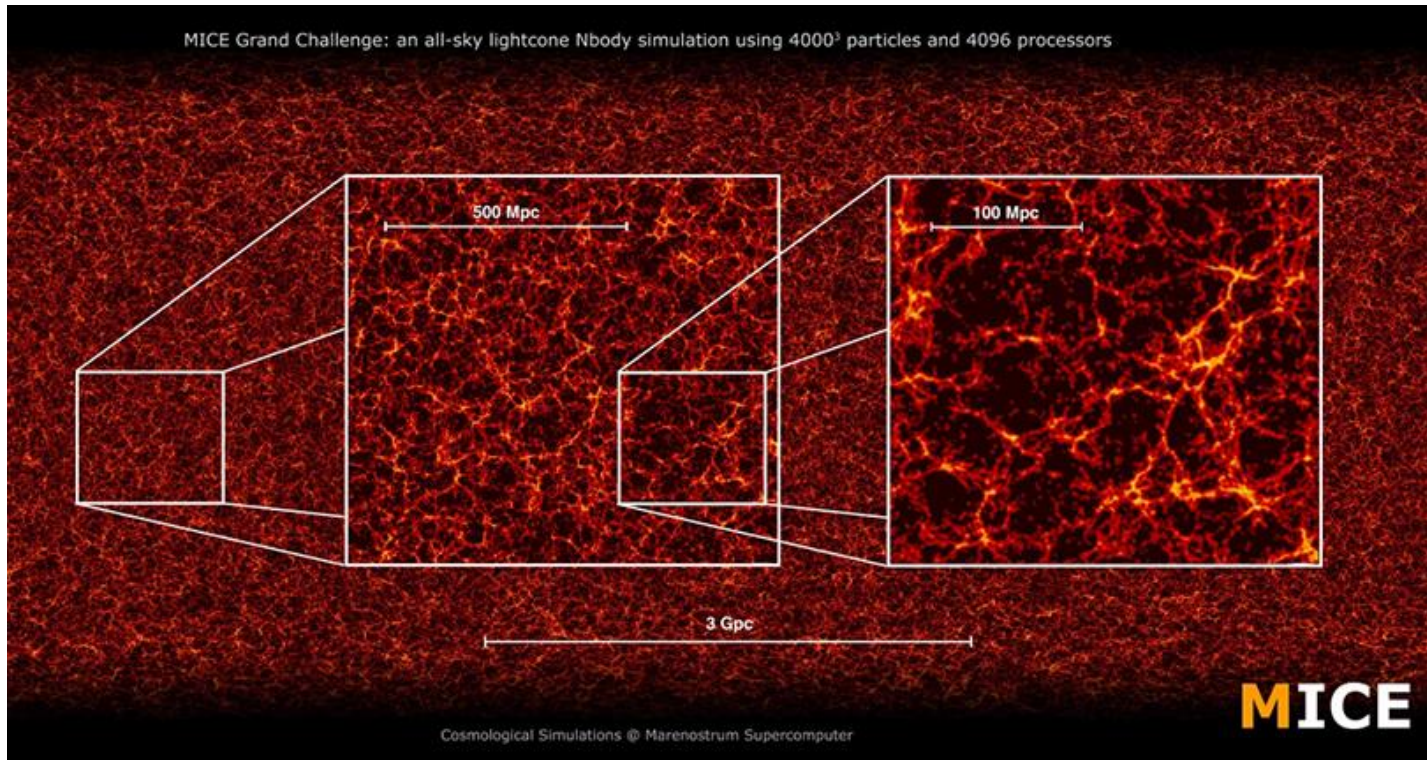
Mock catalogs

MICECAT v2 galaxy mock:

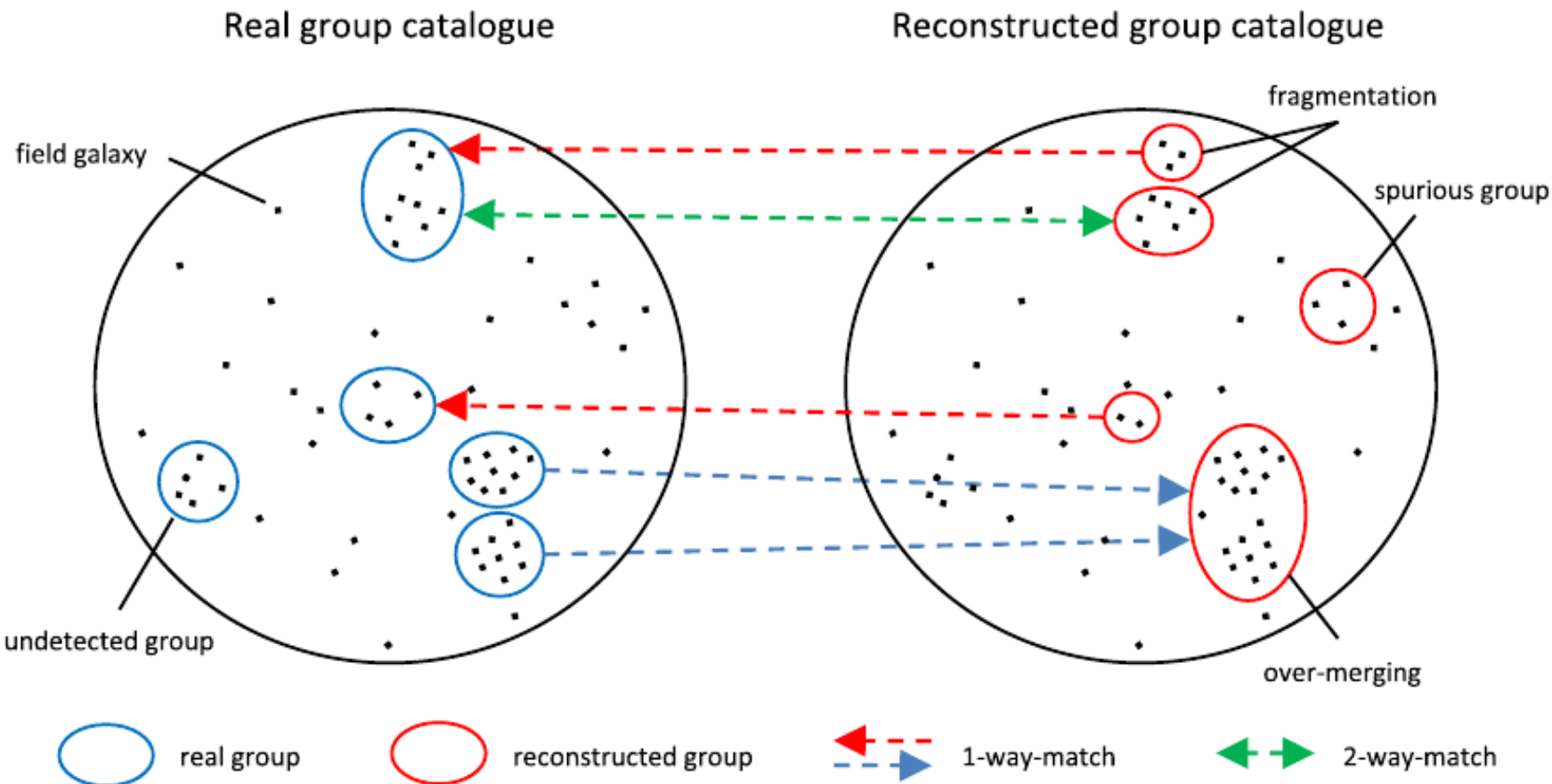
- ~200 million galaxies
- over 5000 sq. deg
- up to a redshift $z=1.4$

We use:

- 10 samples
- 2 sq. deg.
- $R_{ab}=23$ threshold magnitude
- up to a redshift $z=0.8$



Basic statistics



Basic statistics

Completeness:

$$c_1 = \frac{N_{real}^{gr} \rightarrow N_{rec}^{gr}}{N_{real}^{gr}}, \quad c_2 = \frac{N_{real}^{gr} \leftrightarrow N_{rec}^{gr}}{N_{real}^{gr}}$$

Purity:

$$p_1 = \frac{N_{rec}^{gr} \rightarrow N_{real}^{gr}}{N_{rec}^{gr}}, \quad p_2 = \frac{N_{rec}^{gr} \leftrightarrow N_{real}^{gr}}{N_{rec}^{gr}}$$

Galaxy Success Rate:

$$S_{gal} = \frac{S_{real}^{gal} \cap S_{rec}^{gal}}{S_{real}^{gal}}$$

Interloper fraction:

$$f_I = \frac{S_{rec}^{gal} \cap S_{field}^{gal}}{S_{rec}^{gal}}$$

N_{real}^{gr} - the number of real groups, N_{rec}^{gr} - the number of reconstructed groups;
 $N_{real}^{gr} \rightarrow N_{rec}^{gr}$ - the number of associations of real groups to reconstructed groups;
 $N_{rec}^{gr} \rightarrow N_{real}^{gr}$ - the number of associations of reconstructed groups to real groups;
 S_{real}^{gal} - the set of galaxies associated to real groups;
 S_{rec}^{gal} - the set of galaxies associated to reconstructed groups;
 S_{field}^{gal} - the set of real field galaxies.

Filtering algorithm with adaptive kernel

Width of redshift slice: $\Delta z = 0.01 \cdot (1 + z) \pm 25\%$

Density of galaxies distribution:

$$\delta_i = \frac{s}{4/3 \pi R^3}$$

where s is the number of the nearest neighbor, R is the distance for the nearest neighbor.

Mean density in slice:

$$\bar{\delta} = \frac{1}{n} \sum_{i=1}^n \delta_i,$$

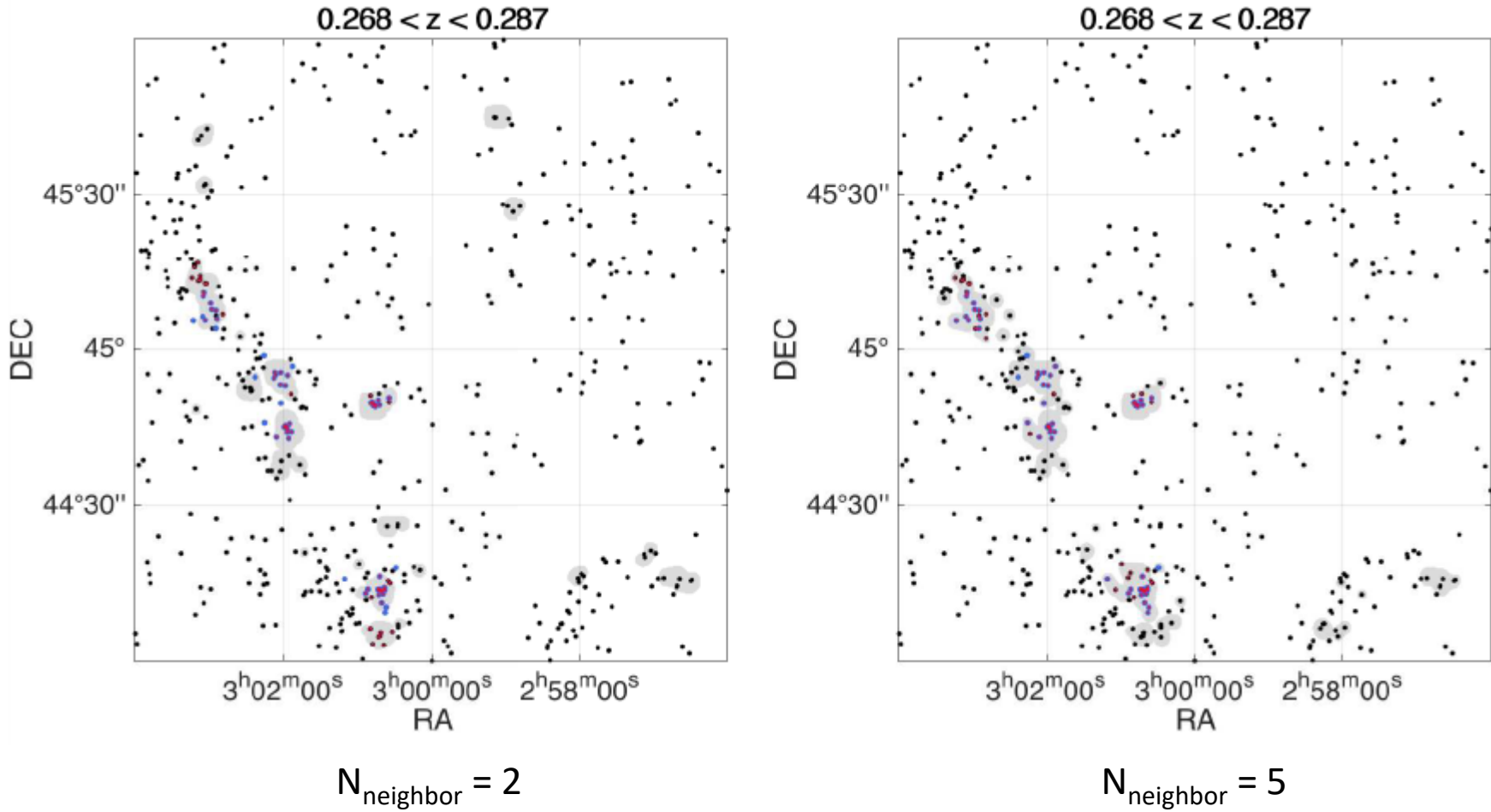
where n is overall number of galaxies in slice.

Density contrast:

$$\sigma_i + 1 = \frac{(\delta_i - \bar{\delta})}{\bar{\delta}} + 1$$

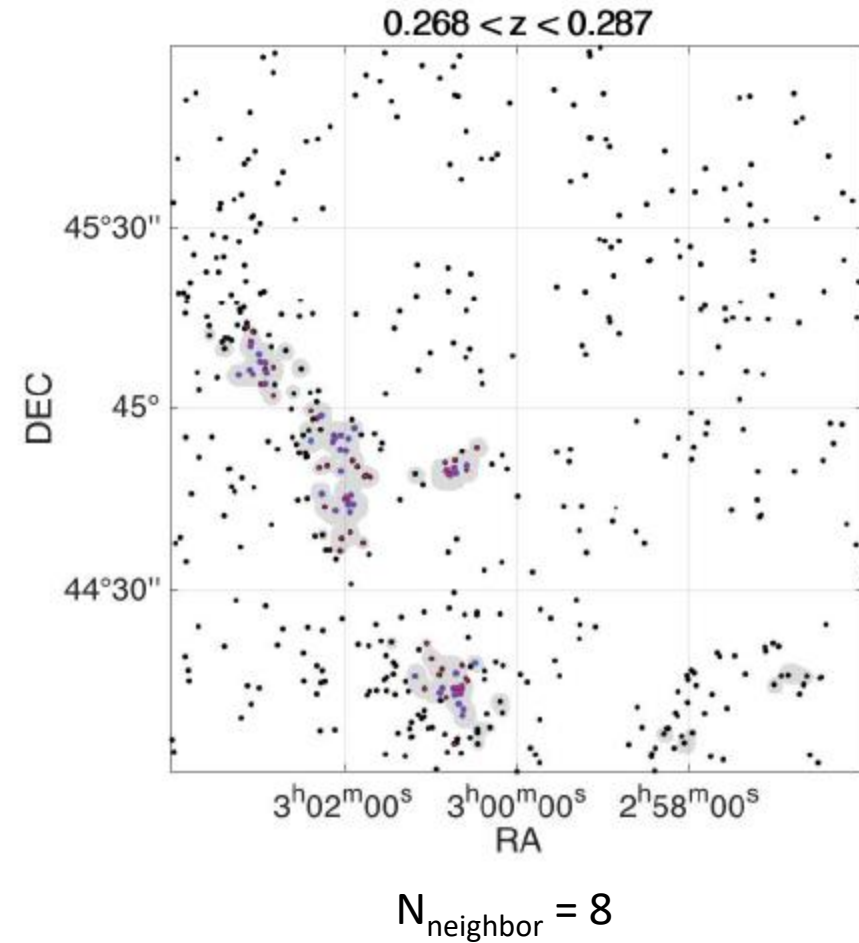
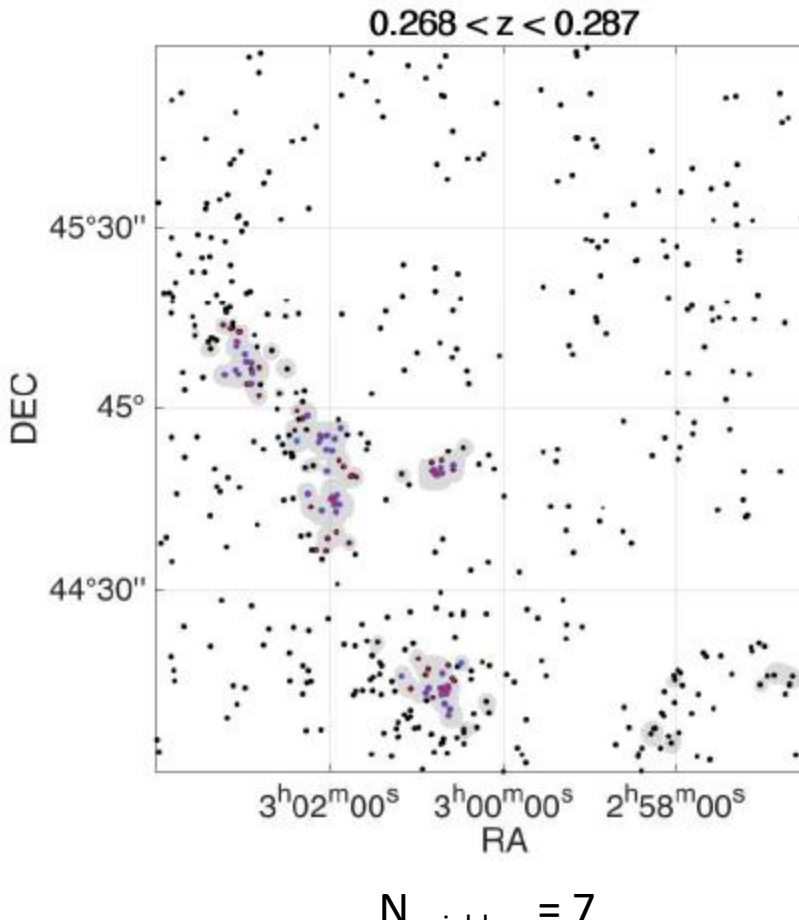


Filtering algorithm with adaptive kernel. 2D

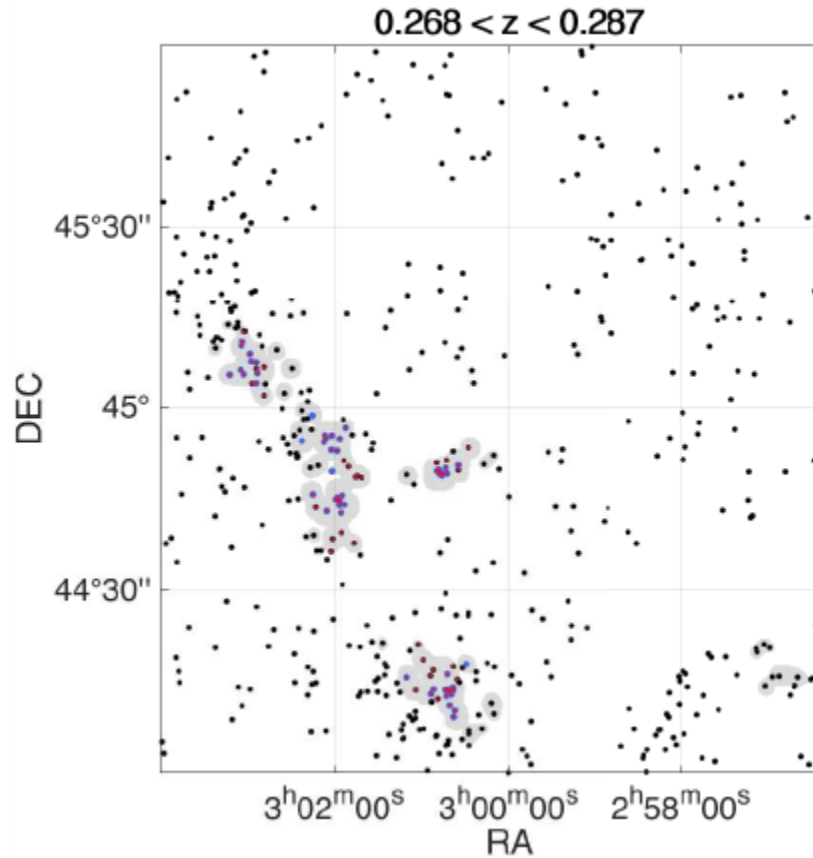




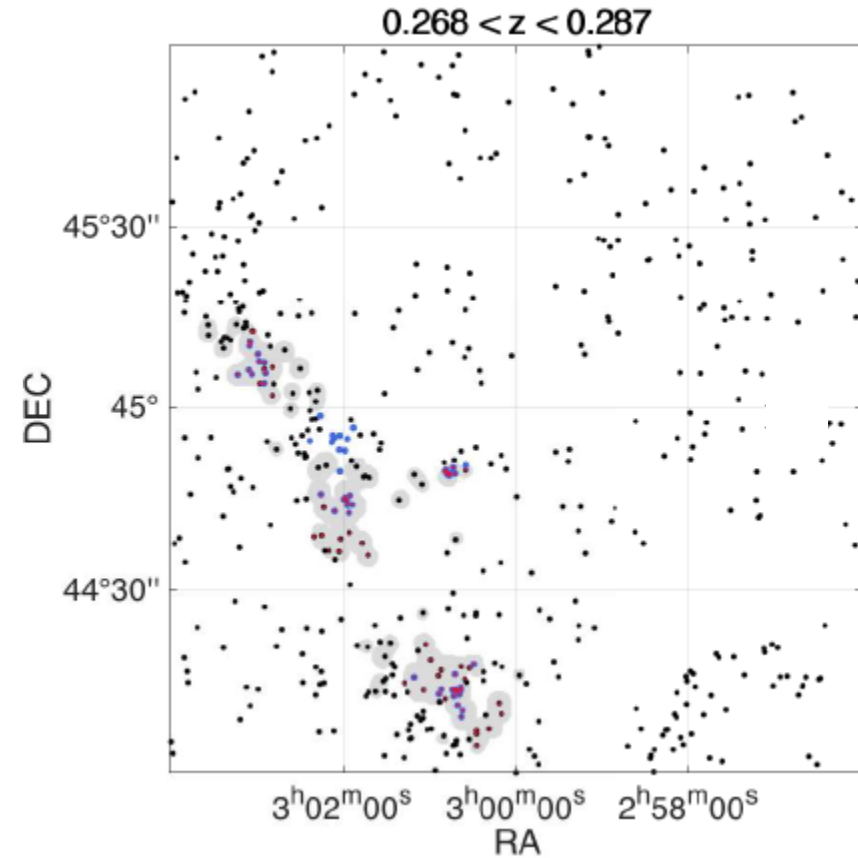
Filtering algorithm with adaptive kernel. 2D



Filtering algorithm with adaptive kernel. 2D



$N_{\text{neighbor}} = 10$

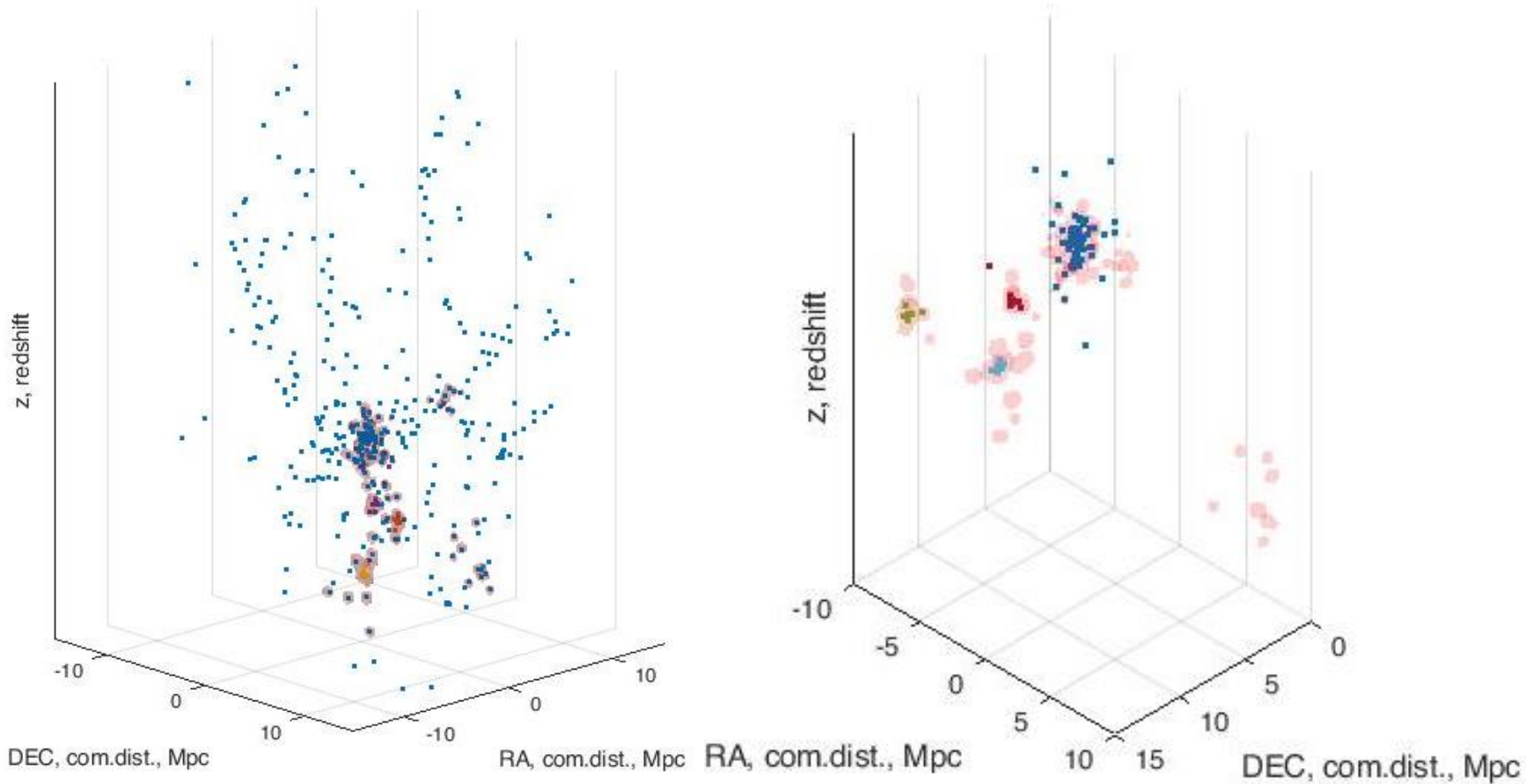


$N_{\text{neighbor}} = 20$



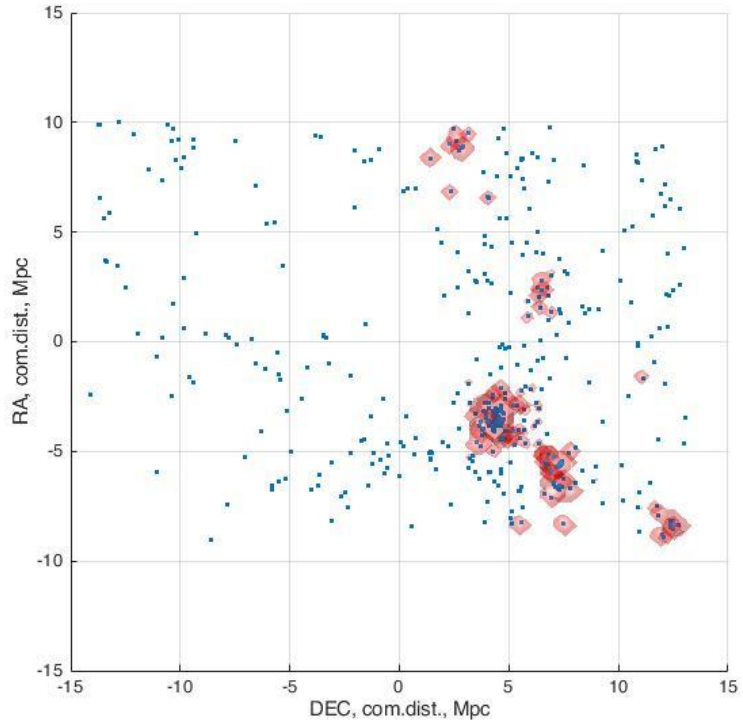
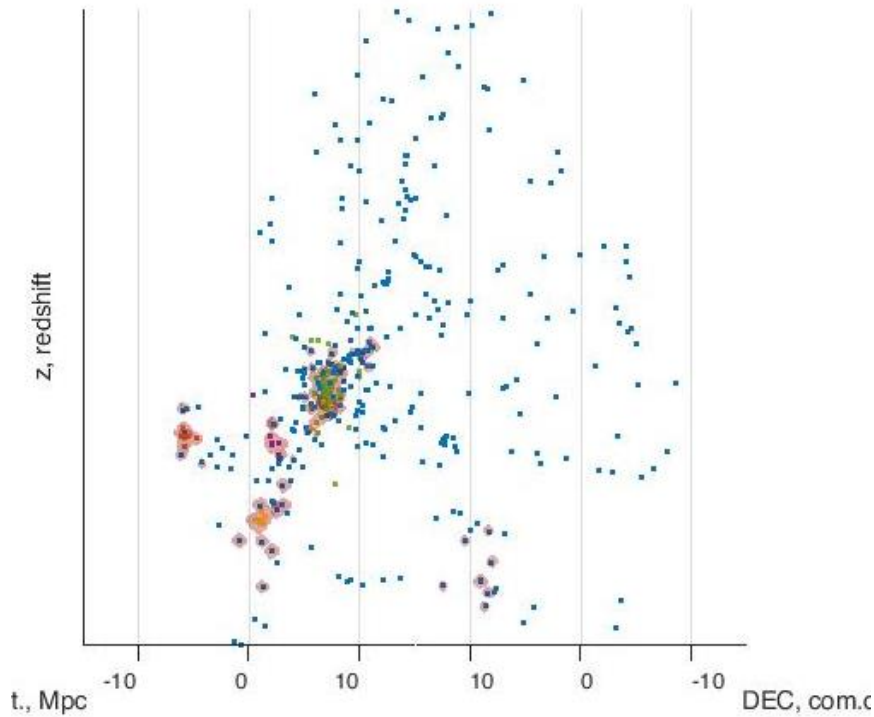
Filtering algorithm with adaptive kernel. 3D

$0.268 < z < 0.287$



Filtering algorithm with adaptive kernel. 3D

$0.268 < z < 0.287$



Voronoi diagrams

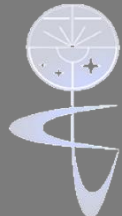
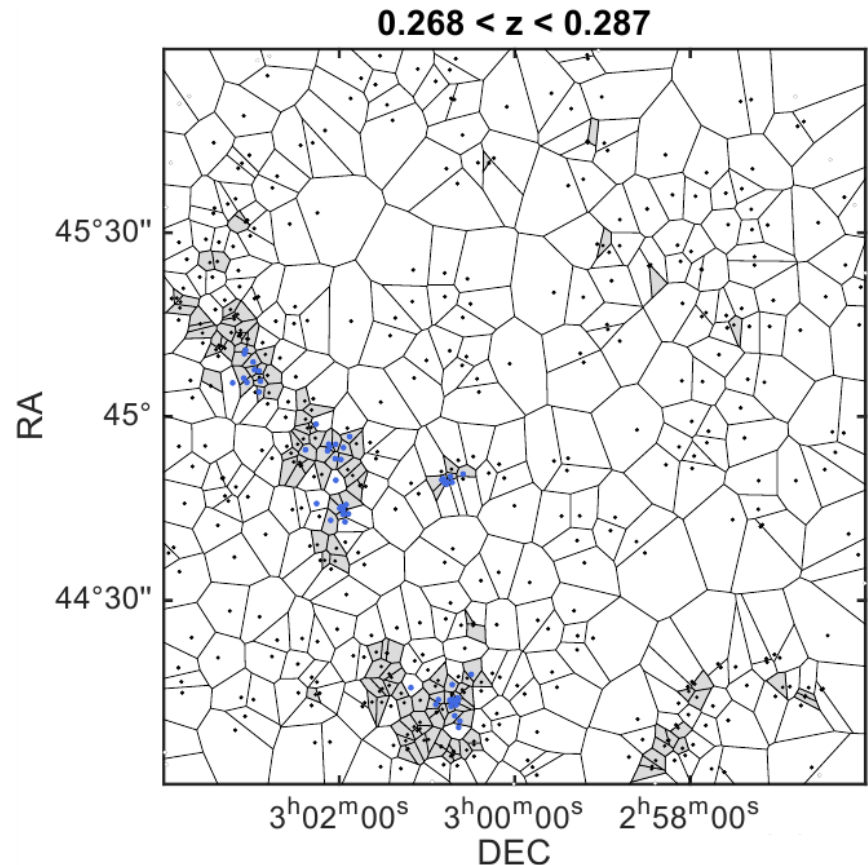
Density contrast:

$$\sigma_i = (\delta_i - \bar{\delta}) / \bar{\delta}$$

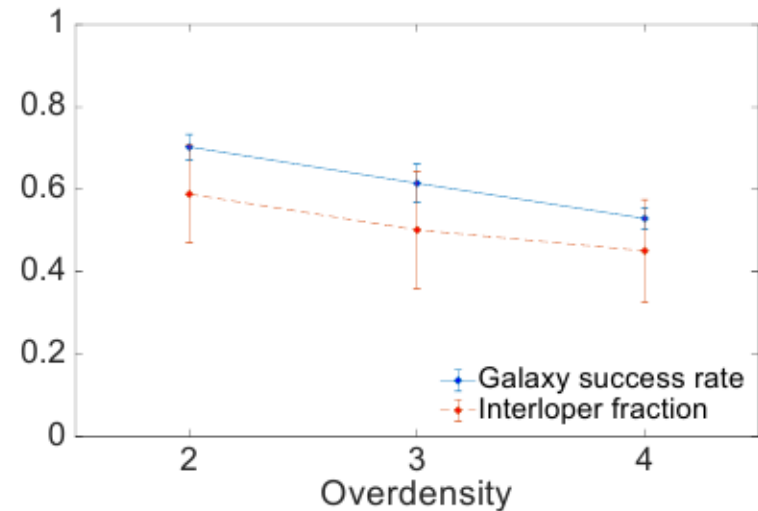
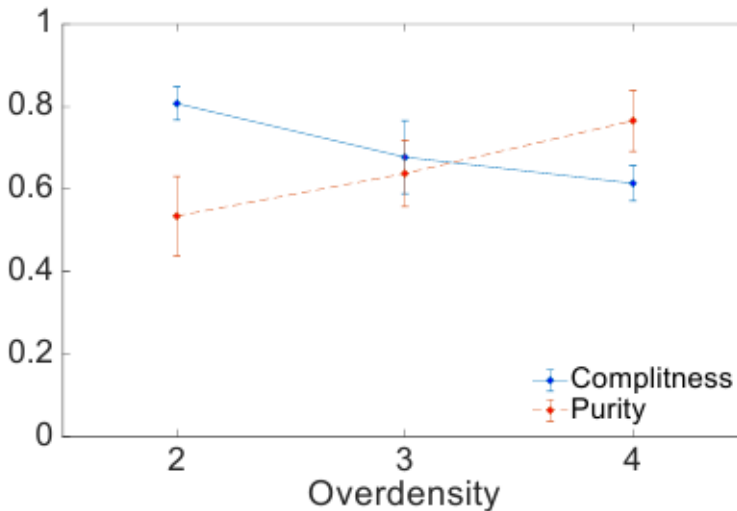
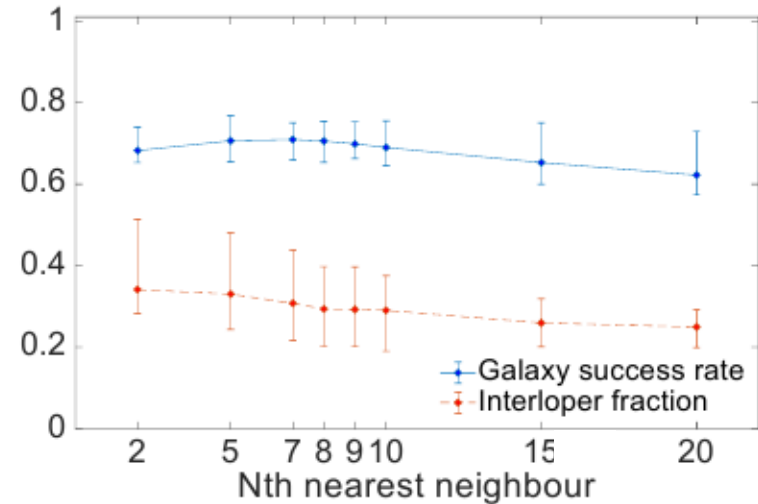
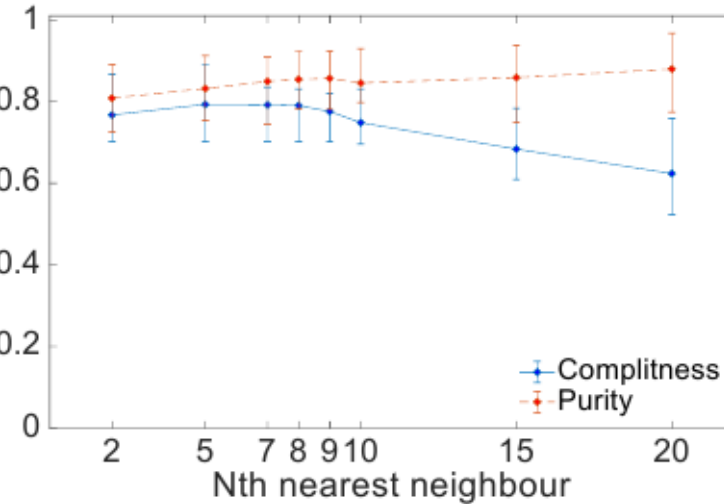
Mean density in slice:

$$\bar{\delta} = \frac{1}{n} \sum_{i=1}^n \frac{1}{A_i},$$

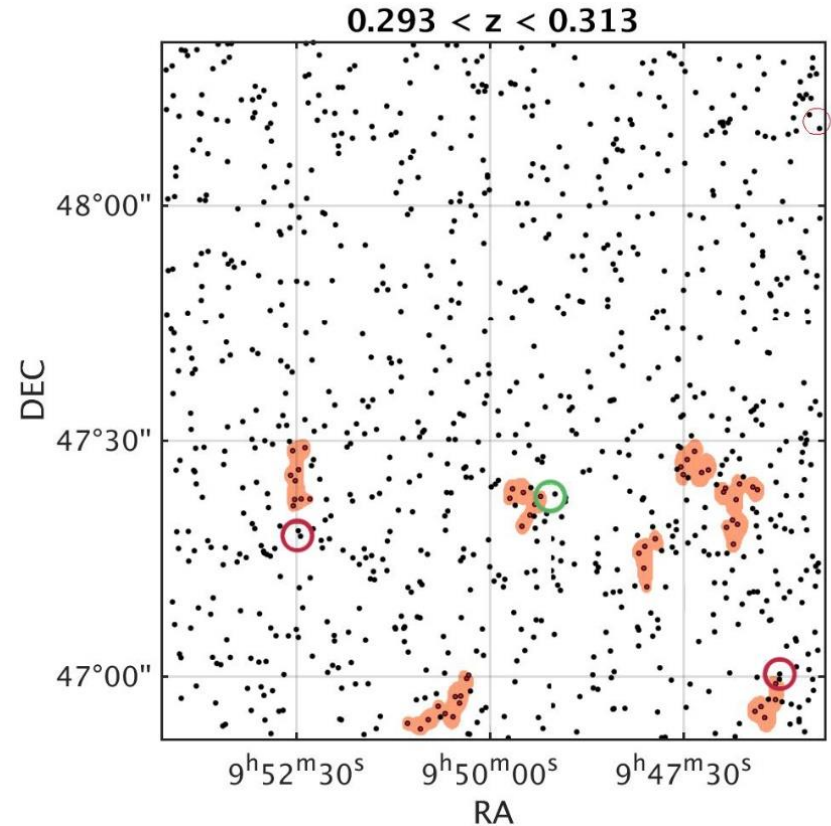
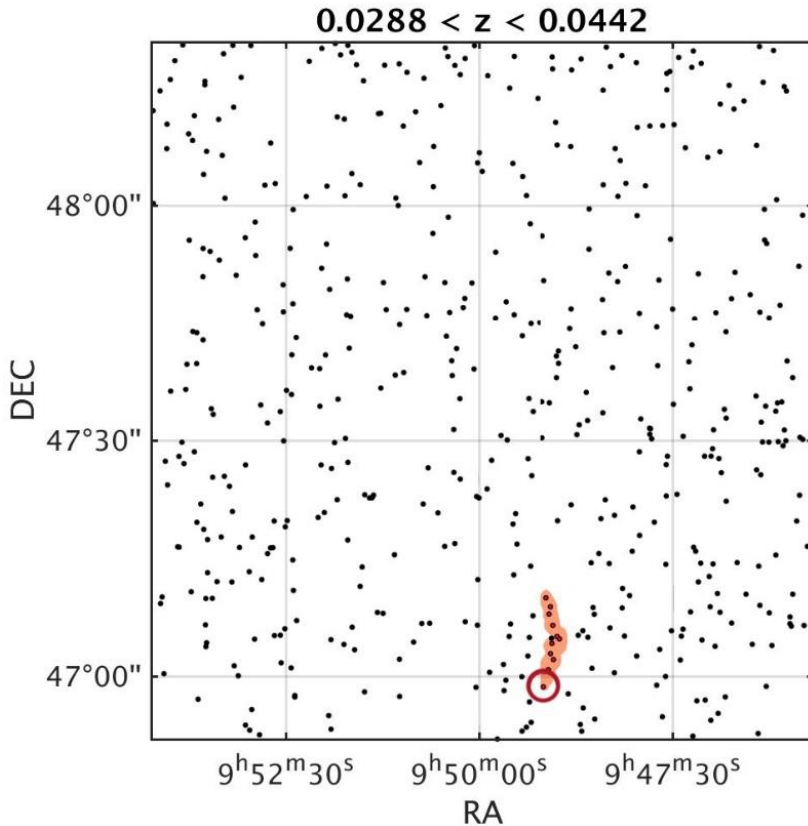
where A_i – is the area of the Voronoi cell around object i and n is the overall number of objects.



Statistics for mock catalogs

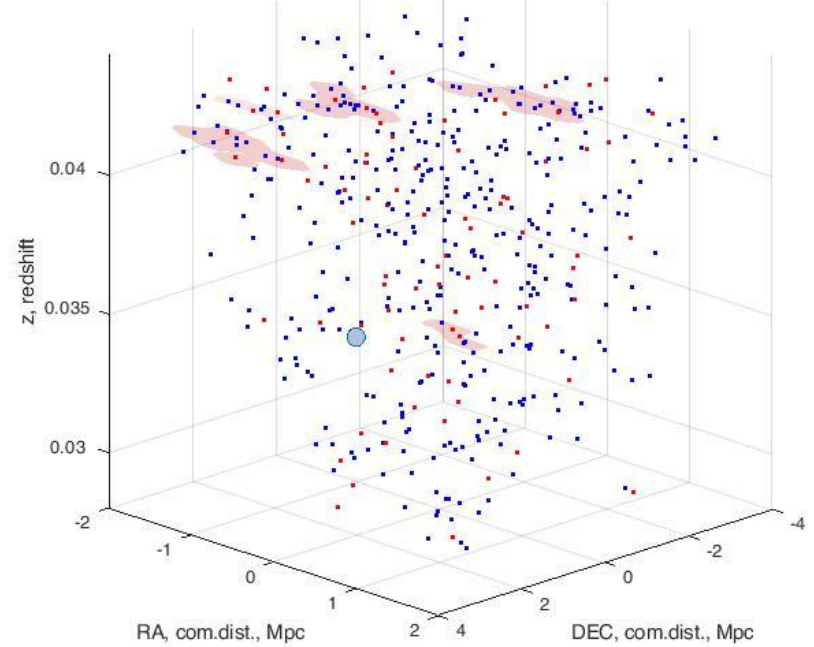
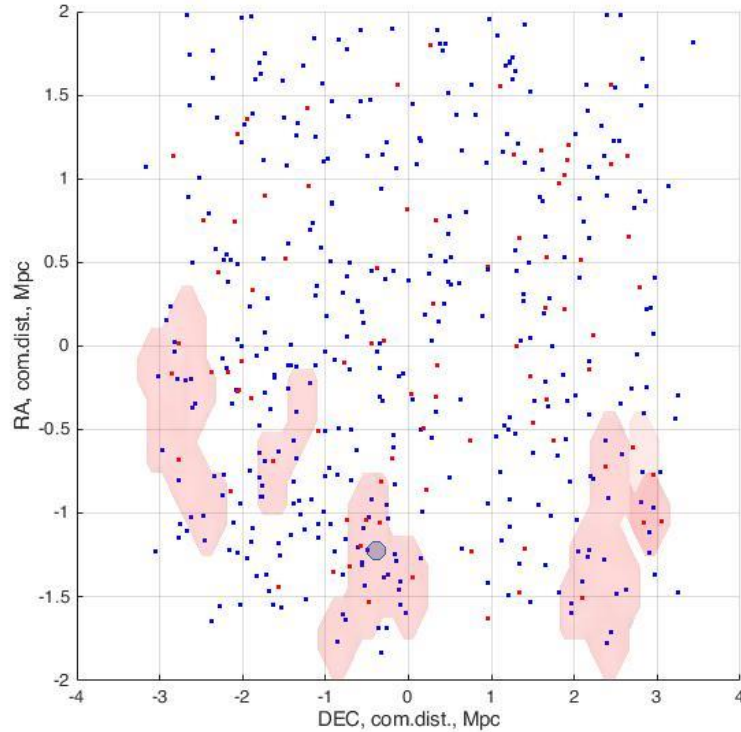


Filtering algorithm with adaptive kernel. 2D. HS 47.5 + 22 field





Filtering algorithm with adaptive kernel. 3D. HS 47.5 + 22 field



Detected cluster MSPM 01061 (Smith +, 2012)
 $z_{\text{spec}} = 0.03282$

Conclusion

- We have tested multilateral analysis methods for large-scale distribution of galaxies.
- We explored the photometric properties of the sample of 36447 galaxies at the field HS47.5-22 and obtained spectral types and photometric redshifts for all objects.
- An accuracy of the redshift allows to determine an accessory of a galaxy to a cluster or a group.
- Based on the our photometric data we obtained maps of the contrast of density distribution with adaptive kernel algorithm (2D, 3D) and Voronoi tessellations (2D).

The main goal of our investigation is a study of the connection between star formation rate in galaxies and their position in the large scale distribution.